Outage Probability of Multi-hop Networks with Amplify-and-Forward Full-duplex Relaying

by

Abhilash Sureshbabu

A Thesis Presented in Partial Fulfillment
of the Requirements for the Degree
Master of Science

Approved September 2016 by the
Graduate Supervisory Committee:

Cihan Tepedelenlioğlu, Chair
Antonia Papandreou-Suppappola
Daniel Bliss

ARIZONA STATE UNIVERSITY

December 2016

ABSTRACT

Full-duplex communication has attracted significant attention as it promises to increase the spectral efficiency compared to half-duplex. Multi-hop full-duplex networks add new dimensions and capabilities to cooperative networks by facilitating simultaneous transmission and reception and improving data rates.

When a relay in a multi-hop full-duplex system amplifies and forwards its received signals, due to the presence of self-interference, the input-output relationship is determined by recursive equations. This thesis introduces a signal flow graph approach to solve the problem of finding the input-output relationship of a multi-hop amplify-and-forward full-duplex relaying system using Mason's gain formula. Even when all links have flat fading channels, the residual self-interference component due to imperfect self-interference cancellation at the relays results in an end-to-end effective channel that is an all-pole frequency-selective channel. Also, by assuming the relay channels undergo frequency-selective fading, the outage probability analysis is performed and the performance is compared with the case when the relay channels undergo frequency-flat fading. The outage performance of this system is performed assuming that the destination employs an equalizer or a matched filter.

For the case of a two-hop (single relay) full-duplex amplify-and-forward relaying system, the bounds on the outage probability are derived by assuming that the destination employs a matched filter or a minimum mean squared error decision feedback equalizer. For the case of a three-hop (two-relay) system with frequency-flat relay channels, the outage probability analysis is performed by considering the output SNR of different types of equalizers and matched filter at the destination. Also, the closed-form upper bounds on the output SNR are derived when the destination employs a minimum mean squared error decision feedback equalizer which is used in outage probability analysis. It is seen that for sufficiently high target rates, full-

duplex relaying with equalizers is always better than half-duplex relaying in terms of achieving lower outage probability, despite the higher RSI. In contrast, since full-duplex relaying with MF is sensitive to RSI, it is outperformed by half-duplex relaying under strong RSI.

ACKNOWLEDGMENTS

I would like to express my gratitude to my supervisor, Dr. Cihan Tepedelenlioğlu, for his support and supervision. His guidance and encouragement have been key in making this work a success.

I would like to extend my thanks to my committee members, Professors Antonia Papandreou-Suppappola and Daniel Bliss. I would also take this opportunity to thank all the faculty members from whom I have learned, including, but not limited to Professors Andreas Spanias, Lina Karam, Junshan Zhang and Yanchao Zhang. This work would not have been successful without the course-work that is the building blocks for my research.

I am also thankful to Professor Fengbo Ren for offering me financial assistantship for most of my graduate study. Thanks to all the staff members of Electrical Engineering department; Sno Kleespies, Ginger Rose and Farah Kiaei, to name just a few, for their extraordinary kindness and infinite patience. They helped me every time I visited them.

My deepest gratitude goes to my father, Sureshbabu M N, mother, Kumudini T R, and family members whose contributions cannot be mentioned in words.

Finally, I am grateful to all my friends and colleagues in the Signal Processing and Communication group. Thanks to Xiaofeng Li, Ruochen Zeng and Ahmed Ewaisha for their help and several useful discussions. Thanks to Vidya, Clara Lobo, Nikitha Satya Murthy, Abdul Roshan Shaik, Ramya Sivaraman, Lakshmi Srinivas, Shrinivas P Shenoy, Naga Shashank Borra, Reethu Gali, Mervyn Rohit, Tarun Gajula, Akhilesh Thyagaturu and many other friends who have supported and encouraged me during the most difficult times of my graduate studies.

TABLE OF CONTENTS

CHAPTER Page

CHAPTER Page

LIST OF FIGURES

Figure Page

Chapter 1

INTRODUCTION

1.1 Wireless Channel Basics

Due to the nature of the wireless channel, the design of wireless networks differ from wired network design. A wireless channel is unpredictable and difficult communication medium. As an information signal propagates through a wireless channel, it experiences random fluctuations in time because of reflections and attenuation if the transmitter, receiver, or surrounding objects are moving. Hence the channel characteristics appear to change randomly with time, making it difficult to design reliable systems with guaranteed performance. Thus, understanding the wireless channel behavior is fundamental to performance analysis. The wireless channel behavior is dependent on multipath fading, the rate of time variation and frequency selectivity.

1.1.1 Multipath Propagation

A radio signal transmitted by a source will encounter multiple objects in the wireless channel environment which produce reflected, diffracted, or scattered copies of the original transmitted signal from the source. These additional copies of transmitted signal called as multipath signal components can be attenuated, delayed and shifted in phase and/or frequency with respect to the line of sight (LOS) component at the destination.

Let the transmitted signal be [1]:

$$x(t) = \Re\left\{u(t)e^{j2\pi f_c t}\right\} , \tag{1.1}$$

where $u(t)$ is the equivalent lowpass signal for $x(t)$ with bandwidth B_u, f_c is the

carrier frequency. Neglecting noise, the corresponding received signal is the sum of the LOS component and all the resolvable multipath components:

$$y(t) = \Re\left\{\sum_{n=0}^{N(t)} \alpha_n(t)u(t-\tau_n(t))e^{j(2\pi f_c(t-\tau_n(t))+\phi_{D_n})}\right\}, \tag{1.2}$$

where $n = 0$ corresponds to the LOS path. $N(t)$ is the number of resolvable multipath components and, for the LOS path and each multipath component, its path length $y_n(t)$ and corresponding delay $\tau_n(t) = y_n(t)/c$, $\phi_{D_n}(t)$ is the Doppler phase shift, and $\alpha_n(t)$ is the amplitude. We say that two multipath components with delay τ_1 and τ_2 are resolvable if $|\tau_1 - \tau_2| \gg B_u^{-1}$. The multipath components which do not satisfy this criterion cannot be separated at the destination because $u(t-\tau_1) \approx u(t-\tau_2)$ and thus are not resolvable.

When these multipath signal components are summed at the destination, it often results in distortion in the received signal.

1.1.2 Small Scale Fading Models

Small scale fading refers to variations in the signal strength over the distances of the order of the carrier wavelength, due to the constructive and destructive interference of multipath components. Channels which undergo small scale fading can be modeled by following statistical channel models:

Rayleigh fading channel: Rayleigh fading is a reasonable model when the transmitted signal undergoes scattering from many scatters present in the transmission environment. If there are sufficiently more scatters then according to the central limit theorem, the channel impulse response will be well-modeled as a Gaussian process irrespective of the distribution of the individual multipath components. If there is no dominant multipath component, then such process will have zero mean. Thus,

the envelope of the channel response will be Rayleigh distributed with distribution

$$p_Z(z) = \frac{2z}{\bar{P}_r} \exp\left(-\frac{z^2}{\bar{P}_r}\right), \quad z \geq 0, \tag{1.3}$$

where, $\bar{P}_r$ is the average received signal power.

Rician fading channel: Rician fading is a reasonable model when the transmitted signal undergoes scattering from many scatters present in the transmission environment and there is a dominant multipath component. The envelope of the channel response will be Rician distributed with distribution

$$p_Z(z) = \frac{2z(K+1)}{\bar{P}_r} \exp\left(-K - \frac{(K+1)\,z^2}{\bar{P}_r}\right) I_0\left(2z\sqrt{\frac{K(K+1)}{\bar{P}_r}}\right), \quad z \geq 0, \tag{1.4}$$

where, $\bar{P}_r$ is the average received power, K is the Rician factor which is the ratio between the power in LOS component to the power in the other multipath components and $I_0(\cdot)$ is the 0^{th} order modified Bessel function of the first kind. When there is no LOS path i.e., K=0 , we have Rayleigh fading and $K = \infty$ corresponds to the non-fading channel. The fading parameter K is, therefore, a measure of the severity of the fading: a small K implies severe fading, a large K implies relatively mild fading.

Nakagami-m fading channel: Rayleigh and Rician distributions can capture the underlying physical properties of the channel models. However, some experimental data does not fit well into either of these distributions. Thus, a more general fading distribution was developed whose parameters can be adjusted to fit a variety of empirical measurements. This distribution is called the Nakagami-m fading distribution [2] and is given by

$$p_Z(z) = \frac{2m^m z^{2m-1}}{\Gamma(m)\bar{P}_r{}^m} \exp\left(\frac{-mz^2}{\bar{P}_r}\right), \quad m \geq 0.5, \tag{1.5}$$

where, $\bar{P}_r$ is the average received power and $\Gamma(\cdot)$ is the Gamma function. Rayleigh fading is a special case of Nakagami-m fading, obtained when m = 1. For m =

$(K+1)^2/(2K+1)$, Nakagami-m fading is approximately Rician fading with parameter K. When $m = \infty$, the channel corresponds to a non-fading channels [3].

1.2 Cooperative Communications and Relaying Strategies

Cooperative communications refer to a scheme where distributed radios interact with each other to transmit information in a wireless network. When cooperative communication is used to leverage spatial diversity available among distributed radios, it results in cooperative diversity. The main motivation here is to improve the reliability of information transferred for a given transmission rate. Also, cooperative communications can be used primarily to increase the transmission rate. Cooperation allows for a trade-off between target performance and required transmitted power, and thus provides additional design options for energy-efficient wireless networks. To illustrate the issues associated with cooperative communications, consider a single source, two relays, and a single destination as shown in Fig.1.1 and Fig.1.2. Generalizations to multi-source, and multi-stage cooperation have also been considered in [4, 5, 6, 7]. Cooperative communication exploits the broadcast nature of the wireless medium and allows radios to jointly transmit information through relays. A relay, by its simplest definition, is a wireless transceiver which can be connected to other relays in parallel and/or series as shown in Fig.1.1 and Fig.1.2 respectively. From Fig.1.1, we can see that the two relays can receive signals resulting from the source transmission, process those received signals, and transmit the signals of their own so as to increase the capacity and improve the reliability of the end-to-end transmissions between the source and destination. From Fig.1.2, we can see that relaying can be performed in multiple stages so that relays as well as the destination benefit from spatial diversity.

Cooperative communication leverages the spatial diversity when multiple transmissions experience fading and/or shadowing. For example, if the source signal expe-

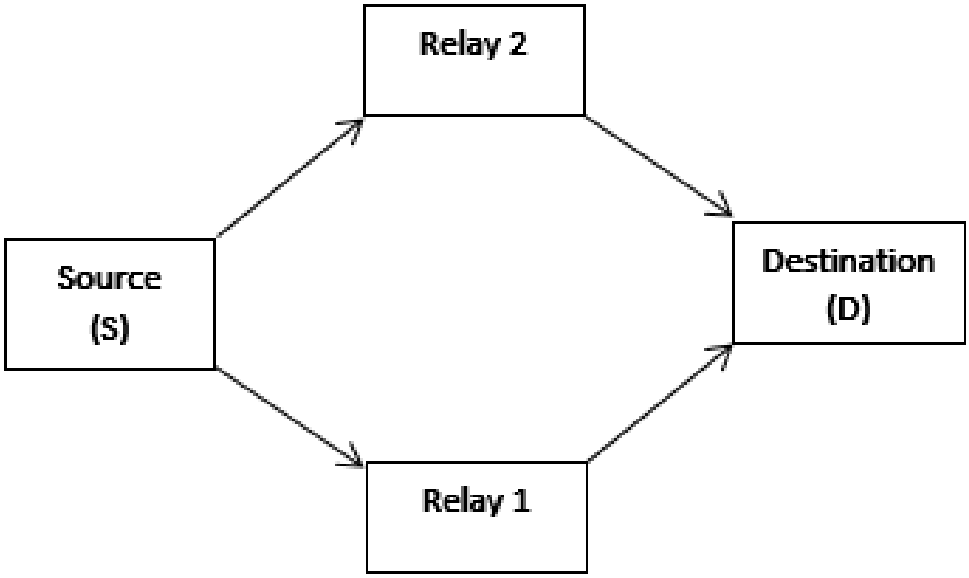

Figure 1.1: Parallel Relays

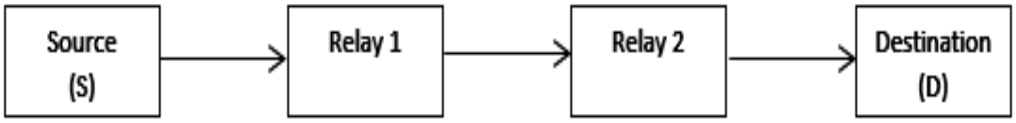

Figure 1.2: Serial Relays

riences a deep fade at the destination, there remains a significant chance that it can be effectively communicated to the destination via one of the other relays.

In communication networks, relays can be used to divert the traffic from congested area of a cellular network to cells with lower traffic. In ad-hoc networks, by employing more number of relays leads to higher network capacity [8],[9]. Relays extend the edge of the cell in a cellular network by forwarding the information signal to the areas where the signal coming directly from the source cannot reach. Relays can also increase cell coverage by filling uncovered territories, particularly in urban areas by eliminating the shadowing effect which is a result of the presence of high buildings [10],[11]. Therefore, relaying systems are efficient in power consumption, and they lead to higher throughput.

To illustrate this, consider a communication system in which a certain information signal has to be transmitted over a distance d. This task can be done in a single-hop, or by dividing the link into N hops, each of length d/N. In the multi-hop case, the relay nodes receive the signal, processes it, and passes it on to the next hop, until the destination is reached. Shorter links require less transmission power and at the same time offer a greater bandwidth, thus motivating the multi-hop approach. Also, if the distance between source and destination is large then the path loss of the end-to-end system is high, consequently, the average SNR of the channel is less. This motivates to use the multiple relays between the source and the destination there by decreasing the path loss.

There are many relaying strategies, each having its own advantages and disadvantages over the others. Relays with different relaying strategies are utilized in different applications depending on the needs. We discuss two important relaying strategies namely, amplify-and-forward relaying and decode-and-forward relaying which were first introduced in [12].

1.2.1 Amplify-and-forward Relaying

Relays with amplify-and-forward relaying strategy amplify the received signal and transmit it towards the destination without any encoding or decoding processes, hence this relaying strategy is also known as non-regenerative relaying [13],[14]. However, the relays transmit the received signal with a different gain, and essentially act as analog repeaters, thereby increasing the system noise level [15]. If relay transmit gain is greater than one, a multi-hop (many relays) system may become unstable due to amplification process at each of the relays. Since amplify-and-forward relaying strategy introduces low processing delays at the relays and is fast due to less computation complexity at the receiver, it is widely used in practical systems [12],[16].

1.2.2 *Decode-and-forward Relaying*

Relays with decode-and-forward relaying strategy decode the received signal and then transmit the re-encoded signal, hence this relaying strategy is also known as regenerative relaying [17],[18]. Relays with decode-and-forward relaying strategy are also referred as digital repeaters, bridges, or routers [15]. Decode-and-forward relaying gives good SNR performance however, it requires high computation power and is not as fast as amplify-and-forward relaying.

1.3 Half-duplex vs. Full-duplex Relaying

A duplex communication system is a point-to-point system where two devices can communicate with one another in both the directions. These systems can be divided into half-duplex and full-duplex relaying systems depending on their ability to transmit and receive at same time [19, 20].

1.3.1 *Half-duplex Relaying*

Consider cooperative networks as shown in Fig.1.1 and Fig.1.2, if the relays operate in half-duplex scheme then they can either receive transmitted signal from the source or transmit their own signal to the destination but not both at the same time. Each relay in the system should wait for its turn to transmit [21]. One way to achieve that is to allocate short time intervals for each of the relays to transmit and receive. By doing that, the communication on each direction looks practically uninterrupted. This is called time-division duplexing (TDD) [21].

1.3.2 Full-duplex Relaying

Consider cooperative networks as shown in Fig.1.1 and Fig.1.2, if the relays operate in full-duplex scheme then they can receive transmitted signal from the source as well as transmit their own signal to the destination at the same time. It can be achieved by allocating different spectrum for each of the relays to transmit on. This is called out-band full-duplex relaying and sometimes called as frequency-division duplexing (FDD) [21]. In contrast, if the same spectrum is allocated for each of the relays to transmit on, it is called as in-band full-duplex relaying [22, 23, 24]. Since the relays will be transmitting and receiving in the same frequency band, the spectral efficiency can be potentially doubled as compared to half-duplex relaying.

In half-duplex relaying, the relays transmit and receive in same frequency band but in different time slots [25]. Consequently, there will be no interference between the transmitted and received signals of the relay. The time to send or receive a symbol doubles as compared to full-duplex relaying. Due to this spectral efficiency loss in half-duplex relaying, half of the time spent on communication is wasted. Therefore full-duplex relaying is more efficient than half-duplex relaying in terms of system capacity and it can potentially provide twice as much capacity as half-duplex relaying [20], [26].

In out-band full-duplex relaying, since the transmitted and received signals at the relays are from different frequency bands, they do not interfere with each other. However, this does not increase the spectral efficiency since different frequency bands are used. In contrast in-band full-duplex relaying doubles the spectral efficiency compared to half-duplex relaying but it has a major disadvantage. The transmitted signal from the relay is also received at the receiver side of the same relay, which is termed as self-interference [27, 28, 29, 30, 31]. Due to this drawback, in-band full-duplex re-

laying systems are not deployed as widely as half-duplex relaying systems [10]. From here on, in-band full-duplex relaying is simply called as full-duplex relaying.

Since 2010, some of the significant experimental results for full-duplex single-input single-output systems have marked a new beginning for full-duplex communications [32, 33, 34, 35, 36]. While before that, it was supposed for a long time that having full-duplex communications is inefficient due to the inherent strong self-interference between the transmitter and receiver of the same full-duplex system. In the two surveys, [22] and [23] on full-duplex communications, challenges and opportunities in wireless communications in PHY and MAC Layers, respectively have been covered.

1.3.3 Self-interference in Full-duplex Relaying

Consider a traditional multi-hop transmission scheme such as in Fig.1.2, let the relays operate in full-duplex relaying scheme. When the Relay 1 receives the signal from source, it simultaneously transmits a signal which it received in previous time slots after some processing. Thus, the signal transmitted by Relay 1 unintentionally interferes with the signal received by Relay 1. This self-interference signal from the transmitter of Relay 1 degrades the system's SINR (signal-to-interference-plus-noise Ratio) performance. Therefore, in order to leverage full-duplex relaying, there should be mitigation of self-interference at the relays.

1.4 Mitigation of Self-interference in Full-duplex Relaying

In the literature, by designing the real model, a group of researchers have focused on interference cancellation techniques, which are divided into three cancellation methods namely, propagation-domain cancellation, analog-domain cancellation and digital-domain cancellation. For bidirectional antennas and MIMO systems, authors in [37] found the lower and upper bounds on the achievable rates for a single

relay model with a direct path between source and destination where the dynamic range limitations were applied. Authors in [32, 33], for the first time, implemented a single transmitter-receiver pair that operates in full-duplex mode. In [38] active analog-domain and digital-domain cancellations were utilized that leads to a total average cancellation of 74 dB. With the assumption that simultaneous reception and transmission in the same frequency band causes an infinite feedback loop in an amplify-and-forward relay and with the channel equalization perspective like in [39], authors in [40] attempted to propose an adaptive cancellation method for MIMO amplify-and-forward full-duplex relays, which mitigated self-interference and channel equalization by means of spectrum restoration. Among these techniques, the self-interference can be canceled by estimating the self-interference channels [41, 42] or be suppressed with the null-space method in MIMO [43]. However, the estimation error and the trade-off between suppression and user rate still lead to RSI. Thus, highly accurate channel state information (CSI) in the presence of RSI is required at the destination to further improve the system performance by canceling RSI. Several works analyze the system performance in the presence of RSI with different criteria such as interference power, outage probability, bit error rate etc. [39, 44, 45]. However, these works do not consider the cancellation of the RSI. Some of the works assume perfect CSI while others assume imperfect CSI without considering how to estimate the channels. [46] gives an overview of the effect of channel estimation errors on the capacity of full-duplex amplify-and-forward relay networks and provides a derivation of a lower bound on the capacity of the system in the presence of channel estimation errors and RSI. Finally, optimal power allocation schemes in maximizing the capacity with joint power constraints are proposed. Excessive channel estimation errors drive full-duplex amplify-and-forward relay into unstable modes and cause capacity reduction [47]. More insight into the self-interference cancellation techniques is given

in the next subsections.

1.4.1 Propagation-domain Self-interference Suppression

Propagation-domain self-interference suppression technique suppresses the self-interference signal by separating the transmitter chain from the receiver chain. This can be achieved by using a combination of cross-polarization [48, 49, 50, 51] and antenna directionality [48, 51] for separate-antenna system or by using a circulator for shared-antenna system. Even though these methods are very effective in suppressing direct-path self-interference, they fail to distinguish between the reflected-path self-interference and the desired received signal. Thus self-interference suppression will not be effective when there is reflect-path self-interference. This motivates in developing channel aware technique to handle reflected path signals.

Transmit beamforming is one among the transmit channel aware propagation-domain self-interference suppression techniques in which the transmit antenna array of full-duplex relay is steered in an attempt to zero the radiation pattern at its receiver antennas. The main drawback of this suppression technique is that, while adjusting the transmit and/or receive patterns to suppress self-interference, the full-duplex relays might accidentally suppress its desired signal.

1.4.2 Analog-circuit-domain Self-interference Cancellation

Analog-circuit-domain self-interference cancellation techniques can be used before analog-to-digital conversion in the receiver-chain circuitry. The transmit signal after the digital-to-analog conversion in transmit-chain is tapped, electronically processed in the analog-circuit domain, and subtracted from the receiver-chain in order to cancel the self-interference. This method can capture the transmitter non-idealities like oscillator-phase noise and high power amplifier distortions because the transmitting

signal is tapped close to the transmitting antennas for the purpose of canceling the self-interference in analog-domain of the receiver chain. Among the analog-circuit-domain self-interference cancellation techniques, channel un-aware techniques aim to cancel direct-path self-interference[33, 48, 52, 53, 54], whereas, channel aware techniques aim to cancel both the direct-path and the reflected-path self-interference [27, 31, 32, 33, 34].

Even though analog-circuit-domain self-interference cancellation techniques circumvent the transmitter non-idealities, these techniques require analog-domain signal processing, which becomes difficult in the case of wideband reflected-path self-interference [22] since it would require adapting an analog filter for each transmit-receive antenna pair in a MIMO system. However, the techniques which tap and process the transmit signal in digital domain have the advantage of using sophisticated adaptive DSP techniques to reflected-path self-interference. However, these cancellation techniques have the disadvantage of reduced cancellation precision due to the presence of analog-circuit non-idealities.

1.4.3 Digital-circuit-domain Self-interference Cancellation

Digital-circuit-domain self-interference cancellation techniques can be used after analog-to-digital conversion in the receiver-chain circuitry by processing the received signal using sophisticated DSP techniques [22]. However, the disadvantage of this technique is that, if the self-interference is strong then the ADC in the receiver circuitry will saturate. Therefore, the ADC's dynamic-range limits the amount of self-interference reduction that is possible. Thus, the self-interference must be sufficiently suppressed before the ADC, using propagation-domain suppression techniques and/or -analog-circuit-domain self-interference cancellation as described in the previous section.

1.5 Previous Works on Multi-hop Networks with Full-duplex Relaying

In this section, we will explore various researches which took place on multi-hop full-duplex relay networks to discuss the problems that are solved in multi-hop full-duplex relay networks and to determine the remaining open problems.

In [55] and [56], a virtual full-duplex relay was proposed by using two half-duplex relays in a novel way. The two relays in each hop transmit data to the next hop in odd and even number of time slots. It means that in a time slot, say an odd number, one of them is transmitting data to the next hop and the other relay is receiving data from the previous hop. Obviously, in each time slot, the relay that is receiving a signal from the previous hop will receive the interference signal coming from the relay that is transmitting data to the next hop. They considered the achievable rates for various coding schemes and compared them with a cut-set upper bound.

Authors in [57] proposed an optimal multi-hop relay selection algorithm that finds the optimal hop count, selects some relays and maximizes transmission rate. With a network security perspective, calculation of the transmit power allocations for full-duplex relays that are obtained by a sub-optimal approach to maximize the lower bound of the achievable secrecy rate using the geometric programming method is done [58]. To achieve the structured cancellation defined in [59], a transmission strategy for multi-hop full-duplex relay network was proposed that is limited to the situations in which the source-to-relay SNR is higher than the relay-to-destination SNR, and limited to the case that the residual self-interference channel coherence time is short. In [60], authors proposed a wireless multi-hop relaying scheme composed of both half-duplex and full-duplex relays. It is assumed that the adjacent relays, in consecutive hops, send interference signals to each other. They have shown that employing all relays in full-duplex mode between source and destination does not

lead to the minimum outage performance.

Diversity-multiplexing trade-off (DMT) of a multiple-input-multiple-output full-duplex single-user multi-hop relay channel is investigated in [61]. It was shown that the DMT upper bound of the channel can be achieved by properly designing space-time codes at the source. However, they did not model any loop interference at full-duplex users, which is a non-trivial assumption in practice.

One of the main problems in full-duplex communications like the secondary collision problem, that occurs while combining wireless full-duplex with multi-hop communication, is avoided by using directional asynchronous full-duplex medium access control (DAFD-MAC) protocol and directional antennas [62]. Authors in [62] also focused on asynchronous timing adjustment because clock synchronization for all nodes in a multi-hop network is an unsettling task. Another problem in full-duplex communications is characterization of the interference relationship between links in the multi-hop full-duplex network. Authors in [63] introduce a novel method for this characterization with the cut-through transmission. By using this method, it is possible to derive simple interference conditions that capture the full-duplex cut-through constraint in a scalable and low-complexity manner. For a two-way relay channel where two sources exchange information through a multi-antenna full-duplex relay, to solve the problems of finding the achievable rate region and maximizing the sum rate, iterative algorithms and 1-D search was proposed [64].

Authors in [65] defined a new parameter named path-loss-to-interference ratio (PLIR), which describes the ratio of the received desired signal power to the received interference power when the transmit powers of the useful and the interference signals are identical. By supposing the general method for calculating the outage probability of multi-hop full-duplex relaying systems employing a decode-and-forward protocol, an outage of the end-to-end communication link occurs if and only if an outage occurs

in at least one of the intermediate links, and they have derived an expression for the overall outage probability.

1.6 Full-duplex Relaying in 5G Standards

Considering the challenges in 5G which includes spectrum management, flexible spectrum allocations, spectrum efficiency and increasing the system throughput, researchers were recently motivated to explore the applicability of full-duplex Radios in 5G [24, 66, 67, 68, 69]. With this regards, in [66] several key design issues in full-duplex network are discussed and some potential solutions are proposed.

Considering a multi-cell scenario, and noticing the fact that by increasing the number of simultaneous transmissions and reception, correspondingly increases the number of interference signals in a small cell, authors in [67] evaluated the performance of full-duplex communication in a dense small cell scenario that has drawn a significant attention of researchers in 5G research. With a practical perspective, authors in [68] addressed the advantages and the disadvantages of potential full-duplex self-interference cancellation techniques such as passive suppression, active analog cancellation, and active digital cancellation. Moreover, an opportunistic decode-and-forward based relay selection scheme is analyzed in the cognitive networks.

In 5G, it is important to guarantee the quality of service (QOS) for wireless full-duplex networks while considering the heterogeneity caused by different types of simultaneous traffic over the wireless full-duplex links. With this aim, authors in [68] formulated the optimization problems to maximize the system throughput subject to heterogeneous statistical delay-bound QoS requirements.

Finally, a group of researchers investigated the applications of self-interference cancellation in 5G and mentioned the self-interference cancellation architectures and costs associated with them [24]. The authors also explored the feasibility of full-duplex

in a small cell and heterogeneous networks.

1.7 Contributions and Outline of Thesis

Full-duplex communication has attracted significant attention as it potentially doubles the spectral efficiency compared to half-duplex. Multi-hop full-duplex networks add new capabilities to cooperative networks by facilitating simultaneous transmission and reception and improving the performance in terms of achieving higher data rates. However, full-duplex communications is not feasible due to the inherent strong loop interference. Therefore, to leverage the advantages of fill-duplex communications, there should be proper self-interference cancellation at the relays.

In multi-hop full-duplex communication, [65] analyzes the outage probability performance of multi-hop decode-and-forward relaying networks where each hop has frequency-flat fading channels. However, to the best of our knowledge, outage probability analysis of multi-hop amplify-and-forward full-duplex relaying systems with frequency-flat or frequency-selective channel is not explored yet. This is due to the fact that it is quite challenging to derive the input-output relationship of multiple full-duplex relays in series suffering residual self-interference.

The thesis is organized as follows. Chapter 2 gives the signal flow graph approach using the Mason's gain formula to solve the problem of finding the input-output relationship of multi-hop full-duplex amplify-and-forward relaying systems. Chapter 3 provides the outage probability analysis of a multi-hop full-duplex amplify-and-forward relaying system. End-to-end output SNR is calculated by employing matched filter and different types of equalizers at the destination, which can be used to perform the outage probability analysis of the end-to-end system. Finally, the conclusion and the scope for future research are presented in Chapter 4.

Chapter 2

MULTI-HOP FULL-DUPLEX AMPLIFY-AND-FORWARD RELAYING

2.1 System Model

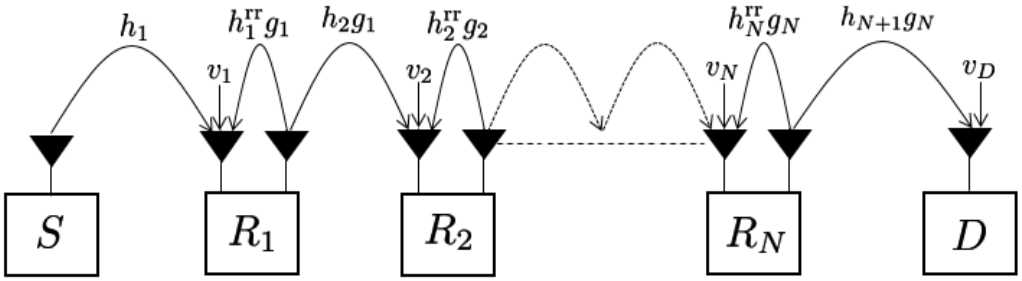

Figure 2.1: System Model with $(N+1)$ hops

A full-duplex multi-hop amplify-and-forward relaying system shown in Fig.2.1, consists of a source node, S, and a destination node, D, connected through N relay nodes, R_1 to R_N, which amplify-and-forward the received signal to the next relay. At time n, S transmits information-bearing signal $x[n]$ to R_1, R_1 amplifies the received signal by a factor $g_1 > 0$ and transmits to R_2, with a processing delay of one symbol period. In general, the relay R_i receives a signal $r_i[n]$, which is the combination of signal transmitted from relay R_{i-1}, denoted as t_{i-1}, its own loop interference signal and the corresponding noise input signal, v_i at relay R_i:

$$r_i[n] = h_i t_{i-1}[n] + h_i^{\mathrm{rr}} t_i[n] + v_i[n], i = 1, \cdots, N, \tag{2.1}$$

and $t_0[n]$=$x[n]$. The transmitted signal $t_i[n]$ by the relay R_i is given by (2.2)

$$t_i[n] = g_i r_i[n-1]. \tag{2.2}$$

The same sequence of amplifying at the i^{th} relay R_i, $i = 1, ..., N$, by a corresponding factor $g_i > 0$ and forwarding to the next relay, R_{i+1}, continues from R_1 to R_N, and eventually the destination D receives the signal incident from R_N, denoted by

$$y[n] = h_{N+1} t_N[n] + v_D[n]. \tag{2.3}$$

We consider frequency-flat Rayleigh fading so that h_i, $i \in \{1, ..., N\}$, are complex Gaussian channel gains between relays R_{i-1} and R_i with zero mean and variance σ_h^2. In a full-duplex relaying system, since reception and transmission occurs at the same time [12],[33], in addition to the information sent from R_{i-1}, R_i also receives an RSI component h_i^{rr}[44],[70]. We assume that all the channels are independent, and both S and relay R_i transmit at normalized average power of unity, additive Gaussian noise terms, v_D, at the destination and v_i, at the relay R_i have an identical variance, σ_v^2. The signal-to-noise ratio (SNR), $\gamma_i = |h_i|^2/\sigma_v^2$, are exponentially distributed random variables with the mean $\Gamma_i = \sigma_h^2/\sigma_v^2$. Furthermore, one can see that the RSI not only makes the overall channel more frequency selective but also introduces colored noise since the noise propagate through multiple relays (multiple filters). In our thesis, we do not perform noise whitening therefore we consider colored noise.

2.2 Amplification Gain at the Relays

We assume that both the source and the relay, R_i, transmits signals $x[n]$ and $t_i[n]$ respectively, at normalized average power of unity [20], i.e., $\mathrm{E}\{|x[n]|^2\} = 1$ and $\mathrm{E}\{|t_i[n]|^2\} = 1$, where $\mathrm{E}\{\cdot\}$ denotes the average over signal and noise distributions. The relay R_i receives a signal $r_i[n]$, given by (2.1), which is the combination of signal transmitted from relay R_{i-1}, denoted as t_{i-1}, its own loop interference signal and the noise input signal, v_i. The transmitted signal $t_i[n]$ by the relay R_i is given by (2.2).

To find amplification factor at R_1, recursive substitution of (2.1) into (2.2) gives,

$$\begin{aligned}
t_1[n] &= g_1 r_1[n-1] \\
&= g_1 \left(h_1 x[n-1] + h_1^{\mathrm{rr}} t_1[n-1] + v_1[n-1]\right) \\
&= g_1 \left(h_1 x[n-1] + v_1[n-1] + h_1^{\mathrm{rr}} g_1 \{h_1 x[n-2] + h_1^{rr} t_1[n-2] + v_1[n-2]\}\right) \\
&= g_1 \sum_{j=1}^{\infty} \left(h_1^{\mathrm{rr}} g_1\right)^{j-1} \left(h_1 x[n-j] + v_1[n-j]\right). \qquad (2.4)
\end{aligned}$$

The instantaneous relay transmit power can be calculated using (2.4) to be,

$$\begin{aligned}
\mathrm{E}\{|t_1[n]|^2\} &= g_1^2 \sum_{j=1}^{\infty} \left(|h_1^{\mathrm{rr}}|^2 g_1^2\right)^{j-1} \left(|h_1|^2 + \sigma_v^2\right) \\
&= g_1^2 \frac{|h_1|^2 + \sigma_v^2}{1 - |h_1^{\mathrm{rr}}|^2 g_1^2}. \qquad (2.5)
\end{aligned}$$

The sum in (2.5) converges, if $g_1^2 < 1/|h_1^{\mathrm{rr}}|^2$. Substituting (2.5) into normalization condition, $\mathrm{E}\{|t_1[n]|^2\} = 1$, amplification factor at relay R_1 after simplification is given to be,

$$g_1 = \left(|h_1|^2 + |h_1^{\mathrm{rr}}|^2 + \sigma_v^2\right)^{-\frac{1}{2}}. \qquad (2.6)$$

To find amplification factor at R_2, again by recursive substitution of (2.1) into (2.2) gives,

$$\begin{aligned}
t_2[n] &= g_2 r_2[n-1] \\
&= g_2 \left(h_2 t_1[n-1] + h_2^{\mathrm{rr}} t_2[n-1] + v_2[n-1]\right) \\
&= g_2 \{h_2 g_1 \left(h_1 x[n-2] + h_1^{\mathrm{rr}} t_1[n-2] + v_1[n-2]\right) + h_2^{\mathrm{rr}} t_2[n-1] + v_2[n-1]\} \\
&= g_2 \sum_{j=1}^{\infty} (h_2^{\mathrm{rr}} g_2)^{j-1} \{h_2 g_1 \left(h_1 x[n-j-1] + h_1^{\mathrm{rr}} t_1[n-j-1] + v_1[n-j-1]\right) + v_2[n-j]\} \\
&= g_2 \sum_{j=1}^{\infty} (h_2^{\mathrm{rr}} g_2)^{j-1} \{h_2 g_1 \sum_{k=0}^{\infty} (h_1^{\mathrm{rr}} g_1)^k \left(h_1 x[n-j-k-1] + v_1[n-j-k-1]\right) + v_2[n-j]\} \\
& \qquad (2.7)
\end{aligned}$$

By noting that the second summation in (2.7) converges if $g_1^2 < 1/|h_1^{\mathrm{rr}}|^2$, the instantaneous relay transmit power can be calculated using (2.4) to be,

$$\mathrm{E}\{|t_2[n]|^2\} = g_2^2 \sum_{j=1}^{\infty} (h_2^{\mathrm{rr}} g_2)^{j-1} \left(\frac{|h_2|^2 g_1^2}{1 - |h_1^{\mathrm{rr}}|^2 g_1^2} \left(|h_1|^2 + \sigma_v^2 \right) + \sigma_v^2 \right). \tag{2.8}$$

The sum in (2.8) converges, if $g_2^2 < 1/|h_2^{\mathrm{rr}}|^2$. Substituting (2.6) into (2.8) and consequently into normalization condition, $\mathrm{E}\{|t_2[n]|^2\} = 1$, after some simplifications, amplification factor at relay R_2 is given to be,

$$g_2 = \left(|h_2|^2 + |h_2^{\mathrm{rr}}|^2 + \sigma_v^2 \right)^{-\frac{1}{2}}. \tag{2.9}$$

Though (2.6) and (2.9) gives the amplification gain of relay R_1 and R_2 respectively only, we can generalize the procedure to find the amplification gain at relay R_i by recursively substituting (2.1) into (2.2) to obtain (2.10). The recursive substitution should be terminated after we get the term $t_0[n]$, since $t_0[n] = x[n]$.

$$t_i[n] = g_i \sum_{j=1}^{\infty} (h_i^{\mathrm{rr}} g_i)^{j-1} \left(h_i t_{i-1}[n-j] + v_i[n-j] \right). \tag{2.10}$$

The sum in (2.10) converges if $|h_i^{\mathrm{rr}}|^2 g_i^2 < 1$. Assuming the signal and noise samples are mutually independent, the instantaneous transit power of relay R_i can be calculated using (2.10). As discussed in the previous sections, the amplification factor g_i is selected such that the instantaneous transmit power in relay is normalized such that $\mathrm{E}\{|t_i[n]|^2\} = 1$. Substituting the expression for $\mathrm{E}\{|t_i[n]|^2\}$ derived from (2.10) into this normalizing condition, we can find the amplifying factor g_i for corresponding relay R_i.

2.3 Mason Gain Formula Approach to Find Input-output Relationship of the Multi-hop Full-duplex Amplify-and-forward Relaying System

In this section, we first discuss the difficulty in finding the input-output relationship of multi-hop full-duplex amplify-and-forward network and then we propose an easy way of finding the input-output relationship based on signal flow graph method by using Mason's gain formula (MGF).

2.3.1 Difficulty in Finding the Input-output Relationship

In full-duplex relaying, we assume that the relays introduce a processing delay of one symbol time due to interference cancellation. Since the relays continuously amplifies-and-forwards previously received symbols, the received symbol at the destination at time n is given by

$$y[n] = h_{N+1}\left(g_N y_{rN}[n-1]\right) + v_D[n], \tag{2.11}$$

where the received signal, $y_{rN}[\cdot]$, at the relay R_N is given by

$$y_{rN}[n] = h_N\left(g_{N-1} y_{r(N-1)}[n]\right) + h_N^{\mathrm{rr}}\left(g_N y_{rN}[n-1]\right) + v_N[n], \tag{2.12}$$

where the received signal, $y_{r(N-1)}[n]$, at the relay R_{N-1} is given by

$$y_{r(N-1)}[n] = h_{N-1}\left(g_{N-2} y_{r(N-2)}[n]\right) + h_{N-1}^{\mathrm{rr}}\left(g_{N-1} y_{r(N-1)}[n-1]\right) + v_{N-1}[n]. \tag{2.13}$$

Due to the RSI, the received signals $y_{rN}[n]$, $y_{r(N-1)}[n]$, $\cdots$, $y_{r1}[n]$ at the relays R_N, R_{N-1} , $\cdots$, R_1, respectively, have a recursive form and thus, are a function of the previously received symbols $x[n]$, $x[n-1]$, $\cdots$. By substituting $y_{rN}[n]$, $y_{r(N-1)}[n]$, $\cdots$, $y_{r1}[n]$ into (2.11) we can find the overall input-output relationship of the network. This method of recursive substitution to find the overall input-output relationship has been done in [39] for the case of two hop (single relay) network. However this approach

of recursive substitution is tedious and complex for the case of networks with more than one relays. In the next sub-sections we propose a signal flow graph method to simplify the procedure of finding the input-output relationship of full-duplex amplify-and-forward networks with any number of relays between source and destination.

2.3.2 Signal Flow Graph Approach

Signal flow graph theory is concerned with the development of a graph theoretic approach to solve a system of linear equations. Two closely related methods proposed by Coates [71] and Mason [72] have appeared in the literature and have served as elegant aids in gaining insight into the structure and nature of solutions of systems of equations. A signal-flow graph, often called as mason graph after Samuel Jefferson Mason, is a specialized directed graph in which nodes represent system variables and arrows represent the functional connection between a pair of nodes.

As discussed earlier, to find the input-output relationship between $x[n]$ and $y[n]$, recursive substitution of (2.2) into (2.1) is done for a single-relay case[39]. This is tedious and complex for systems with multiple relays between source and destination. To avoid this iterative approach, we propose a new method to determine the input-output relationship by showing that the system model shown in Fig. 2.1 can be equivalently represented by a signal-flow graph as shown in Fig.2.2. The transmit antennas of source and destination along with the transmit and receive antennas of the relays are considered as nodes in the signal flow graph. We apply MGF [72, 73] to the signal flow graph given in Fig.2.2, by noting that there is only one forward path with path gain of $h_1 h_2 g_1, ..., h_{i+1} g_i, ..., h_{N+1} g_N z^{-N}$ and N non-touching loops, one at each of the N relays with loop gain $h_i^{\mathrm{rr}} g_i z^{-1}$, where z^{-1} captures the processing delay at each of the N relays.

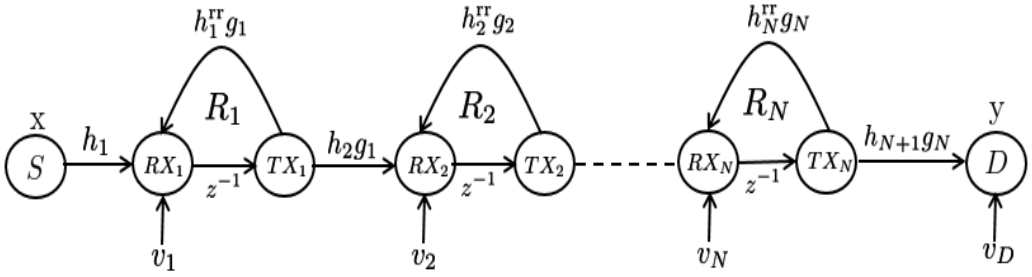

Figure 2.2: Signal-flow Graph

Linearity can be applied to find the input-output relationship of the system including the noise since the output is a linear function of the input and noise processes. This is done by considering two different cases: one by considering only the information-bearing signal as the input while neglecting the noise inputs and the other by considering only the noise terms at respective relays as inputs while neglecting the information-bearing signal input.

2.3.3 Mason Gain Formula

Masons gain rule is a technique for finding an overall transfer function of a network with multiple-inputs and multiple-outputs, which is helpful to simplify a complex network. The purpose of using MGF is the same as that of block reduction. However, MGF is guaranteed to yield a concise result via a direct procedure, where as the process of block reduction can meander. The terminology used for explaining the method of writing the input-output relationship using MGF is,

- Path: A continuous line segments traversed in the direction indicated
- Forward path: A path from input-node to output-node by not going through any of the nodes more than once.
- Loop: A path starting and ending at the same node and not going through any of the intermediate nodes more than once.

- Path gain: Product of gains of all the branches in the path.
- Loop gain: Product of gains of all the branches in the loop.
- Non-touching loops: Two loops which do not have a common node.

The Mason's gain formula is given by,

$$\mathrm{G} = \frac{Y(z)}{X(z)} = \frac{\sum_{k=1}^{M} G_k \Delta_k}{\Delta}. \tag{2.14}$$

$\Delta = 1 - \sum L_i + \sum L_i L_j - \sum L_i L_j L_k + ... + (-1)^m \sum ... + ...$

where,

Δ = the determinant of the signal flow graph

$Y(z)$ = z-transform of the output-node variable

$X(z)$ = z-transform of the input-node variable

G = Transfer function

M = total number of forward paths between $X(z)$ and $Y(z)$

G_k = path gain of the k^{th} forward path between $X(z)$ and $Y(z)$

L_i = loop gain of each closed loop in the system

$L_i L_j$ = product of the loop gains of any two non-touching loops

$L_i L_j L_k$ = product of the loop gains of any three pairwise non-touching loops

Δ_k = the co-factor value of Δ for the k^{th} forward path, with the loops touching the k^{th} forward path removed.

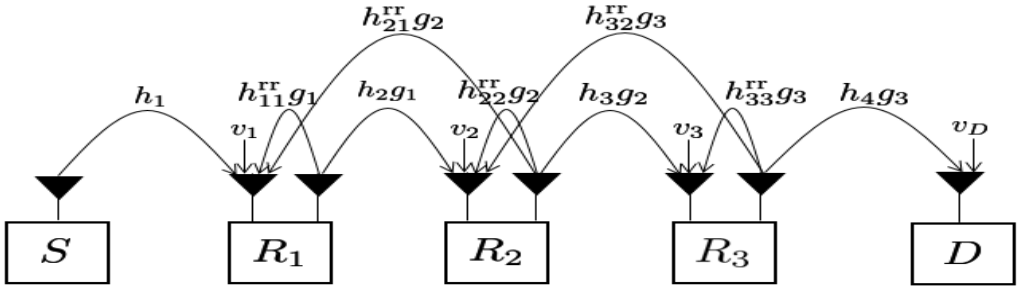

Figure 2.3: Three Relay System with Inter-relay Interference

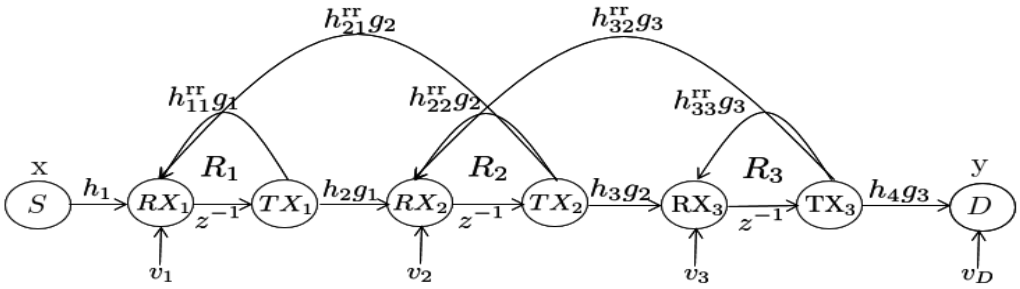

Figure 2.4: Signal-flow Graph of Three Relay System with Inter-relay Interference

Consider a 3-relay system with inter-relay interference as shown in Fig. 2.3, whose corresponding signal-flow graph is given in Fig. 2.4. We can see from the signal-flow graph that, there is only one forward path (M=1), with path gain $G_1 = h_1h_2g_1h_3g_2h_4g_3z^{-3}$. Let the individual loop gains be, $L_1 = h_{11}^{\text{rr}}g_1z^{-1}$, $L_2 = h_{22}^{\text{rr}}g_2z^{-1}$, $L_3 = h_{33}^{\text{rr}}g_3z^{-1}$, $L_4 = h_2g_1h_{21}^{\text{rr}}g_2z^{-2}$ and $L_5 = h_3g_2h_{32}^{\text{rr}}g_3z^{-2}$. The products of two non-touching loops are L_1L_2, L_1L_3, L_2L_3, L_1L_5, L_3L_4 and the products of three non-touching loops are $L_1L_2L_3$.

Since all the loops touch the forward path, Δ_k=1. By noting that the transfer function, G, represents the input-output relationship of the network, since there are four noise inputs, one each at the relays, one symbol input and one output, we can write five input-output relationship equations with respect to each of the five inputs.

Linearity can be applied to find the overall input-output relationship of the system including the noise since the output is a linear function of the input and noise processes. This is done by considering two different cases: one by considering only the information-bearing signal as the input while neglecting the noise inputs and the other by considering only the noise terms at respective relays as inputs while neglecting the information-bearing signal input. The overall transform-domain input-output relationship of the system can be written as,

$$Y(z) = H(z)X(z) + H_{n1}(z)V_1(z) + H_{n2}(z)V_2(z) + H_{n3}(z)V_3(z) + V_D(z). \qquad (2.15)$$

We now proceed to find the effective channels $H(z)$ and $H_{ni}(z)$, $i = 1, 2, 3$, with respect to information symbol and noise at the relay R_i respectively.

- Input-output relationship with respect to symbol input: In this case, noise inputs, v_1, v_2, v_3 and v_D are assumed to be absent. Therefore the signal-flow graph in Fig.2.4 can be modified and it is shown in Fig.2.5, noting that in this case G = $H(z)$, (2.14) reduces to

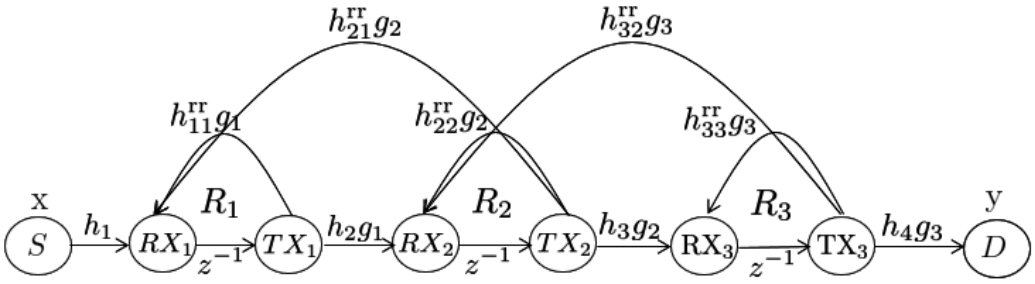

Figure 2.5: Signal-flow Graph of Three Relay System with Inter-relay Interference and with Only Symbol Input

$$H(z) = \frac{h_1 h_2 g_1 h_3 g_2 h_4 g_3 z^{-3}}{1 - (L_1 + L_2 + L_3 + L_4 + L_5) + (L_1L_2 + L_1L_3 + L_2L_3 + L_1L_5 + L_3L_4) - L_1L_2L_3}. \tag{2.16}$$

- Input-output relationship with respect to noise input v_1: In this case, all the inputs other than noise input v_1 are assumed to be absent. Therefore the signal-flow graph in Fig.2.4 can be modified and it is shown in Fig.2.6, noting that in this case G = $H_{n1}(z)$, (2.14) reduces to

$$H_{n1}(z) = \frac{h_2 g_1 h_3 g_2 h_4 g_3 z^{-3}}{1 - (L_1 + L_2 + L_3 + L_4 + L_5) + (L_1L_2 + L_1L_3 + L_2L_3 + L_1L_5 + L_3L_4) - L_1L_2L_3}. \tag{2.17}$$

  It is worth mentioning that $H_{n1}(z) = H(z)/h_1$.

- Input-output relationship with respect to noise input v_2: In this case, all the inputs other than noise input v_2 are assumed to be absent. Therefore the signal-flow graph in Fig.2.4 can be modified and it is shown in Fig.2.7, noting that in

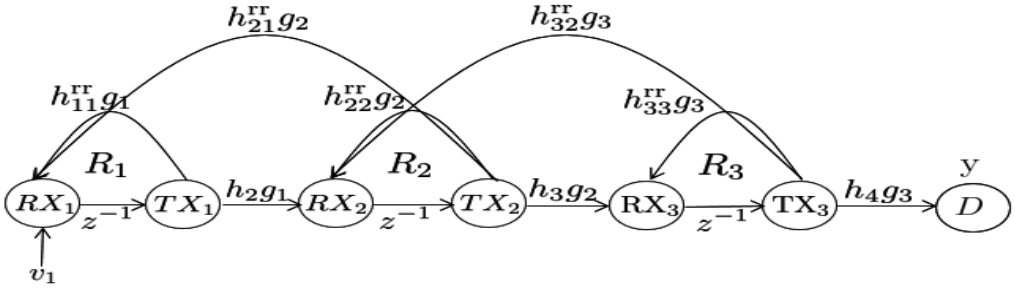

Figure 2.6: Signal-flow Graph of Three Relay System with Inter-relay Interference and with Noise Input v_1

this case G = $H_{n2}(z)$, (2.14) reduces to

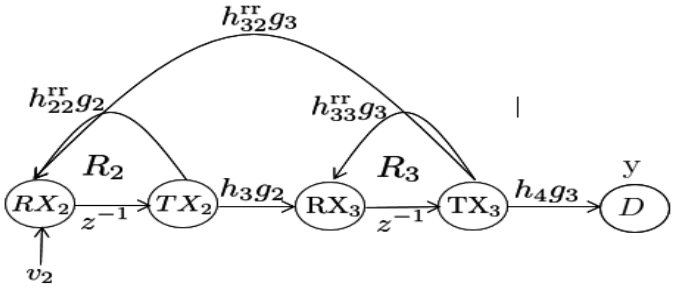

Figure 2.7: Signal-flow Graph of Three Relay System with Inter-relay Interference and with Noise Input v_2

$$H_{n2}(z) = \frac{h_3g_2h_4g_3z^{-2}}{1-(L_2+L_3+L_5)+L_2L_3}. \tag{2.18}$$

- Input-output relationship with respect to noise input v_3: In this case, all the inputs other than noise input v_3 are assumed to be absent. Therefore the signal-flow graph in Fig.2.4 can be modified and it is shown in Fig.2.8, noting that in this case G = $H_{n3}(z)$, (2.14) reduces to

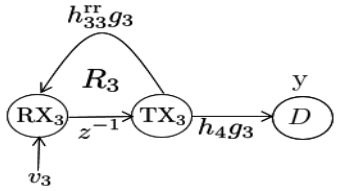

Figure 2.8: Signal-flow Graph of Three Relay System with Inter-relay Interference and with Noise Input v_3

$$H_{n3}(z) = \frac{h_4g_3z^{-1}}{1-L_3}. \tag{2.19}$$

- Input-output relationship with respect to noise input v_D: In this case, all the inputs other than noise input v_D are assumed to be absent. Noting that in this case, (2.14) reduces to, G = $H_{n4}(z)$=1 since the input is same as the output.

2.3.4 Input-output Relationship of the Multi-hop Full-duplex Amplify-and-forward Relaying System

We find the input-output relationship of the multi-hop full-duplex amplify-and-forward relaying system by considering two different cases: one by considering only the information-bearing signal as the input while neglecting the noise inputs and the other by considering only the noise inputs at respective relay as input while neglecting the information-bearing signal input.

Considering the information-bearing signal and neglecting the noise inputs, the transfer function of the system is given by

$$H(z) = \frac{h_1 z^{-N} \prod_{k=1}^{N} h_{k+1} g_k}{1 + \sum_{k=1}^{N} z^{-k} (-1)^k \sum_{A \in \mathbb{S}_k} \prod_{j \in A} h_j^{\mathrm{rr}} g_j}. \tag{2.20}$$

Here $\mathbb{S}_k$ represents the set of subsets of $\{1, 2, ..., N\}$, where k indicates number of elements in subset. If m is the number of subset in $\mathbb{S}_k$ then $(m-1)$ gives the number of summations in the second summation symbol of the denominator in (2.20). Element A of $\mathbb{S}_k$ represents subsets whose element j points to the corresponding self-interference term $h_j^{\mathrm{rr}} g_j$. Here j points to all the elements in subset A. From (2.20), we can see that the denominator has the products of the terms $h_j^{\mathrm{rr}} g_j$ and when N is large, the denominator can be approximated by considering first two terms of the summation

as other terms can be neglected. Consequently, (2.20) reduces to,

$$H(z) = \frac{h_1 z^{-N} \prod_{k=1}^{N} h_{k+1} g_k}{1 - z^{-1} \sum_{j=1}^{N} h_j^{\mathrm{rr}} g_j + z^{-2} \sum_{A \in \mathbb{S}_2} \prod_{j \in A} h_j^{\mathrm{rr}} g_j}. \tag{2.21}$$

Considering the other case without information-bearing signal and only the noise inputs are present, the transfer function corresponding to i^{th} noise input v_i at the relay R_i can be formulated as,

$$H_{ni}(z) = \frac{z^{-(N-i+1)} \prod_{k=i}^{N} h_{k+1} g_k}{1 + \sum_{k=1}^{N} z^{-k} (-1)^k \sum_{A \in \mathbb{S}_{k,i}} \prod_{j \in A} h_j^{\mathrm{rr}} g_j}. \tag{2.22}$$

Here the significance of A and j are same as previous section, but $\mathbb{S}_{k,i}$ represents the set of subsets of $\{i, ..., N\}$ with k elements. Under the same approximation done to obtain (2.21) from (2.20), (2.22) reduces to,

$$H_{ni}(z) = \frac{z^{-(N-i+1)} \prod_{k=i}^{N} h_{k+1} g_k}{1 - z^{-1} \sum_{j=i}^{N} h_j^{\mathrm{rr}} g_j + z^{-2} \sum_{A \in \mathbb{S}_{2,i}} \prod_{j \in A} h_j^{\mathrm{rr}} g_j}. \tag{2.23}$$

The overall transform-domain input-output relationship of the system corresponding to both information-bearing signal and noise signal inputs can be obtained from (2.21) and (2.23) as,

$$Y(z) = H(z)X(z) + \sum_{i=1}^{N} H_{ni}(z) V_i(z) + V_D(z). \tag{2.24}$$

2.4 Impulse Response of Multi-hop Full-duplex Amplify-and-forward Relaying System

For a multi-hop full-duplex amplify-and-forward relaying system, the effective channel for information-signal input at the destination is given by (2.21). Let m_1 and

m_2 be the roots of (2.21), then (2.21) can be written as

$$H(z) = z^{-N} \frac{h_1 \prod_{k=1}^{N} h_{k+1} g_k}{(1 - m_1 z^{-1})(1 - m_2 z^{-1})}. \tag{2.25}$$

Let,

$$H_B(z) = \frac{h_1 \prod_{k=1}^{N} h_{k+1} g_k}{(1 - m_1 z^{-1})(1 - m_2 z^{-1})} = \frac{A}{1 - m_1 z^{-1}} + \frac{C}{1 - m_2 z^{-1}}, \tag{2.26}$$

where, upon solving (2.26), A and C are found to be

$$A = \frac{h_1 \prod_{k=1}^{N} h_{k+1} g_k}{1 - \frac{m_2}{m_1}} \quad \text{and} \quad C = \frac{h_1 \prod_{k=1}^{N} h_{k+1} g_k}{1 - \frac{m_1}{m_2}}. \tag{2.27}$$

Substituting A and C into (2.26) and taking its inverse z-transform, we obtain

$$h_B(n) = \left(\frac{h_1 \prod_{k=1}^{N} h_{k+1} g_k}{1 - \frac{m_2}{m_1}} m_1^n + \frac{h_1 \prod_{k=1}^{N} h_{k+1} g_k}{1 - \frac{m_1}{m_2}} m_2^n \right) u[n]. \tag{2.28}$$

The impulse response of the system, $h[n]$, corresponding to information-bearing signal input can be obtained as,

$$h(n) = h_B(n - N) = \left(\frac{h_1 \prod_{k=1}^{N} h_{k+1} g_k}{1 - \frac{m_2}{m_1}} m_1^{n-N} + \frac{h_1 \prod_{k=1}^{N} h_{k+1} g_k}{1 - \frac{m_1}{m_2}} m_2^{n-N} \right) u[n - N]. \tag{2.29}$$

The effective channel for noise source at the destination is given by (2.23). Let m_3 and m_4 be the roots of (2.23), then (2.23) can be written as

$$H_{ni}(z) = z^{-(N-i+1)} \frac{\prod_{k=i}^{N} h_{k+1} g_k}{(1 - m_3 z^{-1})(1 - m_4 z^{-1})}. \tag{2.30}$$

Let,

$$H_{Bi}(z) = \frac{\prod_{k=i}^{N} h_{k+1}g_k}{(1-m_3z^{-1})(1-m_4z^{-1})} = \frac{E}{1-m_3z^{-1}} + \frac{F}{1-m_4z^{-1}}, \tag{2.31}$$

where, upon solving (2.31), E and F are found to be

$$E = \frac{\prod_{k=i}^{N} h_{k+1}g_k}{1-\frac{m_4}{m_3}} \quad \text{and} \quad F = \frac{\prod_{k=i}^{N} h_{k+1}g_k}{1-\frac{m_3}{m_4}}. \tag{2.32}$$

Substituting E and F into (2.31) and taking its inverse z-transform, we obtain

$$h_{Bi}(n) = \left(\frac{\prod_{k=i}^{N} h_{k+1}g_k}{1-\frac{m_4}{m_3}} m_3^n + \frac{\prod_{k=i}^{N} h_{k+1}g_k}{1-\frac{m_3}{m_4}} m_4^n \right) u[n]. \tag{2.33}$$

The impulse response,$h_{ni}(n)$ corresponding to noise input v_i, can be obtained as,

$$\begin{aligned} h_{ni}(n) &= h_{Bi}(n-(N-i+1)) \\ &= \left(\frac{\prod_{k=i}^{N} h_{k+1}g_k}{1-\frac{m_4}{m_3}} m_3^{n-(N-i+1)} + \frac{h_2\prod_{k=i}^{N} h_{k+1}g_k}{1-\frac{m_3}{m_4}} m_4^{n-(N-i+1)} \right) u[n-(N-i+1)]. \end{aligned} \tag{2.34}$$

Using (2.20) and (2.22), one can find the effective channel with respect to input signal and noise respectively, which determine the end-to-end SNR of the system. In the next chapter, by using (2.20) and (2.22) we derive the end-to-end SNR using which we perform the outage probability analysis.

2.5 Conclusions

The recursive substitution method to find the input-output relationship of a multi-hop full-duplex amplify-and-forward relaying system is tedious for complex networks

involving many relays with inter-relay interference. We introduced the signal flow graph approach using the Mason's gain formula which provides a simple method to find the input-output relationship of any complex multi-hop full-duplex amplify-and-forward relaying system. To demonstrate this, we took an example of a three relay system with inter-relay interference and derived the effective channel equation for both the information signal input and the noise inputs. Also, we derived the generalized input-output relationship along with the channel impulse responses for the information signal and the noise inputs for a multi-hop full-duplex amplify-and-forward relaying system.

Chapter 3

OUTAGE PROBABILITY ANALYSIS OF FULL-DUPLEX AMPLIFY-AND-FORWARD RELAYING SYSTEM

In this chapter, the outage probability of the multi-hop full-duplex amplify-and-forward relays is analyzed by considering matched filter and different types of equalizers at the destination. A general procedure to perform the outage probability analysis of a multi-hop system is discussed and then the outage probability analysis for the case of the two and three-hop systems is done. Also, the upper bounds on the output SNR at the output of MMSE-DFE at the destination by assuming perfect interference cancellation at one of the relays are derived.

3.1 Matched Filtering at the Output

Matched filtering is a process for detecting a known signal that is embedded in noise by maximizing the signal-to-noise ratio (SNR) of the signal being detected with respect to the noise. The matched filter performs correlation of a known signal with an unknown signal to detect the presence of a signal in the unknown signal.

3.2 Equalization at the Output

The full-duplex multi-hop relays suffer from self-interference, making the effective end-to-end channel as frequency-selective due to multipath propagation. Consequently, the transmitted symbols undergo inter-symbol interference (ISI) [74]. Viterbi algorithm can be used to counter-act ISI but it has large computation complexity, making the use of Viterbi algorithm expensive to implement practically. However, one can use sub-optimal channel equalization approaches to equalize the channel and

reduce ISI to allow correct recovery of the transmitted symbols. The equalizers can be linear or non-linear, we consider two types of linear equalizers namely zero-forcing equalizer, minimum mean squared error equalizer and a non-linear equalizer namely minimum mean squared error decision feedback equalizer [75].

3.2.1 Zero-forcing Equalizer (ZFE)

Zero-forcing equalizer approximates the inverse of the channel with a linear filter to eliminate ISI. The output SNR of the Zero-forcing equalizer is given by (3.1),

$$\gamma_{\text{eq}} = \left(\int_{-\frac{1}{2}}^{\frac{1}{2}} \frac{S_n(f)}{S_s(f)} \, \mathrm{d}f \right)^{-1}. \tag{3.1}$$

One can see that when the signal spectral characteristics possess any zeros, the output SNR of the ZFE goes to zero. Therefore, the performance of ZFE will be bad when the signal spectral characteristics possess null or takes on small values. This is because of the fact that when the equalizer tries to eliminate ISI, it also enhances the additive noise.

3.2.2 Minimum Mean Squared Error (MMSE) Equalizer

If e is the error signal, which is the difference between the transmitted information signal and the estimate of that signal, MMSE equalizer uses a filter which minimizes $E\left[|\mathrm{e}|^2\right]$. The output SNR of the linear MMSE equalizer is given by (3.2),

$$\gamma_{\text{eq}} = -1 + \left(\int_{-\frac{1}{2}}^{\frac{1}{2}} \frac{1}{1 + \left(\frac{S_s(f)}{S_n(f)} \right)} \, \mathrm{d}f \right)^{-1}. \tag{3.2}$$

3.2.3 MMSE Decision Feedback Equalizer (MMSE-DFE)

MMSE-DFE is a type of non-linear equalizer whose performance is generally better than that of linear equalizers. The MMSE-DFE equalizer consists of two filters,

a feedforward filter and a feedback filter. The received signal is the input to the feedforward filter and the sequence of decisions on previously detected symbols are the input to the feedback filter. The feedback filter is used to remove the ISI from the present estimated symbol from the previously detected symbols. This equalizer is considered to be a nonlinear since the detector feeds hard decisions to the feedback filter. The output SNR of such type of MMSE-DFE is given by (3.3),

$$\gamma_{\text{eq}} = -1 + \exp\left(\int_{-\frac{1}{2}}^{\frac{1}{2}} \log\left(1 + \frac{S_s(f)}{S_n(f)}\right) \, \mathrm{d}f\right). \tag{3.3}$$

Using the independence of the noise at the relays, the power spectral density of the signal, $S_s(f)$, and the power spectral density of the noise, $S_{n_i}(f)$, can be derived from (2.20) and (2.22) by using the relationships,

$$S_s(f) = |H(e^{j2\pi f})|^2, \tag{3.4}$$

$$S_{n_i}(f) = |H_{\text{ni}}(e^{j2\pi f})|^2. \tag{3.5}$$

Overall power spectral density of noise inputs at all the relays, $S_n(f)$, can be derived from the relation,

$$S_n(f) = \sigma_v^2 \left[1 + \sum_{i=1}^{N} S_{n_i}(f)\right]. \tag{3.6}$$

Equations (3.4) and (3.6) can be determined for any multi-hop system and upon substituting into (3.1), (3.2) and (3.3), one can find the output SNR of the respective equalizer. If the resulting SNR is below a threshold SNR Γ_T, the end-to-end system is considered to be in outage, this threshold SNR is related to target rate, R_T, of the system according to Shannon capacity formula as,

$$R_T = \log_2(1 + \Gamma_T) \quad \text{bps/Hz}. \tag{3.7}$$

3.3 Outage Probability Analysis of Multi-hop Amplify-and-forward Half-duplex and Full-duplex Relaying Systems with Flat Fading Channels

In the previous section we discussed the general procedure to finding the output SNR of a multi-hop amplify-and-forward full-duplex system with N number of hops using which one can perform outage probability analysis. By using the procedure we discussed, in this section, we derive the bounds on outage probability of a two-hop systems with matched filter and MMSE-DFE at the destination. We also derive the bounds on the output SNR expressions of a three-hop system with MMSE-DFE.

3.3.1 Outage Probability Analysis of Two-hop System

Consider a two-hop (N=1 relay) system without direct link as shown in Fig. 3.1. The amplification factor at the relay is given by (2.6). When the relay operates in half-duplex scheme then the instantaneous received SNR is given by [12]

$$\begin{aligned}\gamma_{HD} &= \frac{g^2|h_1|^2|h_2|^2}{\left(g^2|h_2|^2+1\right)\sigma^2} \\ &= \frac{\gamma_1\gamma_2}{\gamma_1+\gamma_2+1}\,. \end{aligned} \tag{3.8}$$

When the relay operates in full-duplex scheme, equations (2.20) and (2.22) can be used to obtain the expressions for $H(z)$ and $H_{\mathrm{n}}(z)$ as,

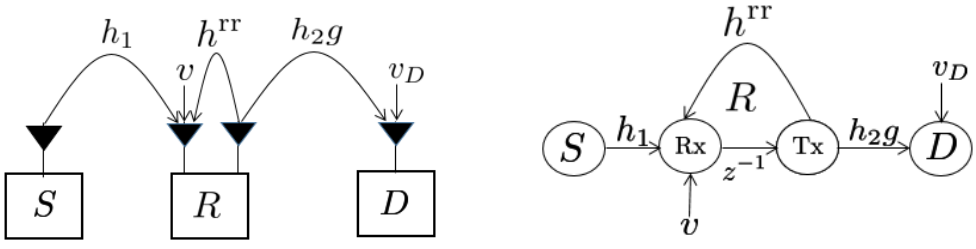

(a) Block diagram (b) Signal-flow graph

Figure 3.1: System Model of Two-hop System

$$H(z) = \frac{h_1 h_2 g z^{-1}}{1 - h^{\mathrm{rr}} g z^{-1}} \quad , \qquad H_n(z) = \frac{h_2 g z^{-1}}{1 - h^{\mathrm{rr}} g z^{-1}}. \tag{3.9}$$

Linearity can be applied to find the input-output relationship of the system including the noise since the output is a linear function of the input and noise processes. By modifying (2.24), one can obtain an end-to-end input-output relationship of the two-hop system as,

$$Y(z) = H(z)X(z) + H_n(z)V(z) + V_D(z). \tag{3.10}$$

Taking inverse z-transform of $Y(z)$,

$$\begin{aligned} y[n] &= h[n] * x[n] + h_n[n] * v[n] + v_D[n] \\ &= h_1 h_2 g (h^{\mathrm{rr}} g)^{n-1} u[n-1] * x[n] + h_2 g (h^{\mathrm{rr}} g)^{n-1} u[n-1] * v[n] + v_D[n] \\ &= \sum_{k=1}^{\infty} h_1 h_2 g (h^{\mathrm{rr}} g)^{k-1} x[n-k] + \sum_{k=1}^{\infty} h_2 g (h^{\mathrm{rr}} g)^{k-1} v[n-k] + v_D[n]. \end{aligned} \tag{3.11}$$

When the destination performs matched filtering (MF) with respect to the strongest tap of the channel, treating all the other taps due to RSI as noise, we can upper-bound the output SNR of MF as,

$$\begin{aligned} \gamma_{\mathrm{MF}} &= \frac{|h_1|^2 |h_2|^2 g^2}{\underbrace{|h_1|^2 |h_2|^2 g^2 \frac{|h^{\mathrm{rr}}|^2 g^2}{1 - |h^{\mathrm{rr}}|^2 g^2}}_{\text{RSI}} + \underbrace{\left(|h_2|^2 g^2 \frac{1}{1 - |h^{\mathrm{rr}}|^2 g^2} + 1 \right) \sigma^2}_{\text{noise amplification}}} \\ &= \frac{\gamma_1 \gamma_2}{\gamma_1 + \gamma^{\mathrm{rr}} (\gamma_2 + 1) + \gamma_2 + 1} \qquad (3.12) \\ &\leq \frac{\gamma_1 \gamma_2}{\gamma_1 + \gamma^{\mathrm{rr}} \gamma_2 + \gamma_2 + 1}. \qquad (3.13) \end{aligned}$$

From [13], using the cumulative density function of the SNR γ_{MF}, the outage

probability is lower-bounded by

$$\begin{aligned}\Pr\left(\frac{\gamma_1\gamma_2}{\gamma_1+\gamma_2+\gamma_2\gamma^{\mathrm{rr}}+1}\leq\Gamma_T\right)&=\Pr\left(\gamma^{\mathrm{rr}}\geq\frac{\gamma_1\gamma_2-\Gamma_T\left(\gamma_1+\gamma_2+1\right)}{\gamma_2\Gamma_T}\right)\\&=1-\Pr\left(\gamma^{\mathrm{rr}}\leq\underbrace{\frac{1}{\gamma_2\Gamma_T}(\gamma_1(\gamma_2-\Gamma_T)-\Gamma_T(\gamma_2+1))}_{=\psi}\right)\\&=1-\int\int_{\psi\geq0}\left(1-e^{-\frac{\psi}{\Gamma^{\mathrm{rr}}}}\right)\frac{1}{\Gamma_1}e^{-\frac{\gamma_1}{\Gamma_1}}\frac{1}{\Gamma_2}e^{-\frac{\gamma_2}{\Gamma_2}}\,\mathrm{d}\gamma_1\,\mathrm{d}\gamma_2.\end{aligned}$$

We can divide the integration region $\psi\geq0$ with integration limits $\Gamma_T\leq\gamma_2<\infty$ and $\gamma_{\mathrm{lt}}\leq\gamma_1<\infty$, where $\gamma_{\mathrm{lt}}=\Gamma_T(\gamma_2+1)/\left(\gamma_2-\Gamma_T\right)$

$$\begin{aligned}\Pr\left(\frac{\gamma_1\gamma_2}{\gamma_1+\gamma_2+\gamma_2\gamma^{\mathrm{rr}}+1}\leq\Gamma_T\right)&=1-\int_{\gamma_2=\Gamma_T}^{\infty}\int_{\gamma_1=\gamma_{\mathrm{lt}}}^{\infty}\left(1-e^{-\frac{\psi}{\Gamma^{\mathrm{rr}}}}\right)\frac{1}{\Gamma_1}e^{-\frac{\gamma_1}{\Gamma_1}}\frac{1}{\Gamma_2}e^{-\frac{\gamma_2}{\Gamma_2}}\,\mathrm{d}\gamma_1\,\mathrm{d}\gamma_2\\&=1-\int_{\gamma_2=\Gamma_T}^{\infty}\frac{1}{\Gamma_1\Gamma_2}e^{-\frac{\gamma_2}{\Gamma_2}}\,\mathrm{d}\gamma_2\int_{\gamma_1=\gamma_{\mathrm{lt}}}^{\infty}\left(1-e^{-\frac{\psi}{\Gamma^{\mathrm{rr}}}}\right)e^{-\frac{\gamma_1}{\Gamma_1}}\,\mathrm{d}\gamma_1.\end{aligned}\tag{3.14}$$

For the purpose of simplification, let us consider the RHS of (3.14),

$$\begin{aligned}&1-\int_{\gamma_2=\Gamma_T}^{\infty}\frac{1}{\Gamma_1\Gamma_2}e^{-\frac{\gamma_2}{\Gamma_2}}\,\mathrm{d}\gamma_2\int_{\gamma_1=\gamma_{\mathrm{lt}}}^{\infty}\left(1-e^{-\frac{\psi}{\Gamma^{\mathrm{rr}}}}\right)e^{-\frac{\gamma_1}{\Gamma_1}}\,\mathrm{d}\gamma_1\\&=1-\int_{\gamma_2=\Gamma_T}^{\infty}\frac{1}{\Gamma_1\Gamma_2}e^{-\frac{\gamma_2}{\Gamma_2}}\,\mathrm{d}\gamma_2\left[\int_{\gamma_1=\gamma_{\mathrm{lt}}}^{\infty}e^{-\frac{\gamma_1}{\Gamma_1}}\,\mathrm{d}\gamma_1-\int_{\gamma_1=\gamma_{\mathrm{lt}}}^{\infty}e^{-\left(\frac{\psi}{\Gamma^{\mathrm{rr}}}+\frac{\gamma1}{\Gamma_1}\right)}\,\mathrm{d}\gamma_1\right]\\&=1-\int_{\gamma_2=\Gamma_T}^{\infty}\frac{1}{\Gamma_1\Gamma_2}e^{-\frac{\gamma_2}{\Gamma_2}}\,\mathrm{d}\gamma_2\left[-\Gamma_1e^{-\frac{\gamma_1}{\Gamma_1}}\Big|_{\gamma_1=\gamma_{\mathrm{lt}}}^{\infty}+\frac{1}{\frac{1}{\Gamma^{\mathrm{rr}}\gamma_2\Gamma_T}\left(\gamma_2-\Gamma_T\right)+\frac{1}{\Gamma_1}}e^{-\left(\frac{\psi}{\Gamma^{\mathrm{rr}}}+\frac{\gamma1}{\Gamma_1}\right)}\Big|_{\gamma_1=\gamma_{\mathrm{lt}}}^{\infty}\right]\\&=1-\int_{\gamma_2=\Gamma_T}^{\infty}\frac{1}{\Gamma_1\Gamma_2}e^{-\frac{\gamma_2}{\Gamma_2}}\,\mathrm{d}\gamma_2\left[\Gamma_1e^{-\frac{\Gamma_T(\gamma_2+1)}{\Gamma_1(\gamma_2-\Gamma_T)}}-\frac{1}{\frac{1}{\Gamma^{\mathrm{rr}}\gamma_2\Gamma_T}\left(\gamma_2-\Gamma_T\right)+\frac{1}{\Gamma_1}}e^{-\frac{\Gamma_T(\gamma_2+1)}{\Gamma_1(\gamma_2-\Gamma_T)}}\right]\\&=1-\int_{\gamma_2=\Gamma_T}^{\infty}\frac{1}{\Gamma_2}e^{-\frac{\gamma_2}{\Gamma_2}}\,\mathrm{d}\gamma_2\left[\frac{\Gamma_1\left(\gamma_2-\Gamma_T\right)}{\Gamma_1\left(\gamma_2-\Gamma_T\right)+\gamma_2\Gamma^{\mathrm{rr}}\Gamma_T}e^{-\frac{\Gamma_T(\gamma_2+1)}{\Gamma_1(\gamma_2-\Gamma_T)}}\right]\\&=1-\int_{z=0}^{\infty}\frac{1}{\Gamma_2}e^{\frac{-\Gamma_T-z}{\Gamma_2}}\left[\frac{\Gamma_1z}{\Gamma_1z+\Gamma^{\mathrm{rr}}\Gamma_T\left(z+\Gamma_T\right)}e^{-\frac{\Gamma_T(\Gamma_T+z+1)}{\Gamma_1z}}\right]\,\mathrm{d}z\\&=1-\frac{e^{-\frac{\Gamma_T}{\Gamma_2}}e^{-\frac{\Gamma_T}{\Gamma_1}}}{\Gamma_2}\int_{z=0}^{\infty}e^{-\frac{z}{\Gamma_2}}e^{-\frac{\Gamma_T^2+\Gamma_T}{\Gamma_1z}}\frac{\Gamma_1z}{\Gamma_1z+\Gamma^{\mathrm{rr}}\Gamma_T\left(z+\Gamma_T\right)}\,\mathrm{d}z,\end{aligned}\tag{3.15}$$

where, $z=\gamma_2-\Gamma_T$ and when

$$\frac{\Gamma_1z}{\Gamma_1z+\Gamma^{\mathrm{rr}}\Gamma_T\left(z+\Gamma_T\right)}\simeq\frac{\Gamma_1}{\Gamma_1+\Gamma^{\mathrm{rr}}\Gamma_T}\,,\tag{3.16}$$

(3.15) is reduced to,

$$\Pr(\gamma_{MF} \leq \Gamma_T) \geq 1 - \frac{e^{-\frac{\Gamma_T}{\Gamma_2}} e^{-\frac{\Gamma_T}{\Gamma_1}}}{\Gamma_2} \int_{z=0}^{\infty} e^{-\frac{z}{\Gamma_2}} e^{-\frac{\Gamma_T^2+\Gamma_T}{\Gamma_1 z}} \frac{\Gamma_1}{\Gamma_1 + \Gamma^{\mathrm{rr}}\Gamma_T} \, \mathrm{d}z. \tag{3.17}$$

Using [76, Eq. 3.471.9], (3.17) can be simplified to get

$$\begin{aligned} \Pr(\gamma_{MF} \leq \Gamma_T) &\geq 1 - e^{-\frac{\Gamma_T}{\Gamma_1}} e^{-\frac{\Gamma_T}{\Gamma_2}} \frac{\Gamma_1}{\Gamma_1 + \Gamma^{\mathrm{rr}}\Gamma_T} \xi_2 K_1(\xi_2) \\ &\approx 1 - e^{-\frac{\Gamma_T}{\Gamma_1}} e^{-\frac{\Gamma_T}{\Gamma_2}} \left(1 - \underbrace{\frac{\Gamma^{\mathrm{rr}}\Gamma_T}{\Gamma_1 + \Gamma^{\mathrm{rr}}\Gamma_T}}_{=L_{MF}} \right). \end{aligned} \tag{3.18}$$

Note that in the above equation, $\xi_2 = 2\sqrt{\left(\Gamma_T + \Gamma_T^2\right)/\Gamma_1\Gamma_2}$ and $K_n(x) = \int_0^{\infty} e^{-x\cosh(t)} \cosh(nt) \, \mathrm{d}t$ is the n-th order modified Bessel function of the second kind. We can see that the outage performance degradation due to RSI, denoted by $\mathbb{L}_{MF}$ in (3.18), does not goes to zero even when Γ_2 tends to infinity. This is due to the fact that, when RSI is treated as noise, increasing γ_2 amplifies the total amount of interference at the same time which can be seen in (3.13).

However, observing that the RSI in the relays also contains useful information about the transmitted symbol, the destination can potentially achieve higher SNR by equalizing the entire channel. Since the performance of MMSE-DFE is better than other equlaizer [77], we consider MMSE-DFE equalizer at the destination to derive the equations for outage probability of the network. $S_s(f)$ and $S_n(f)$ can be derived from $H(z)$ and $H_{\mathrm{n}i}(z)$ respectively, as discussed earlier and the ratio $S_s(f)/S_n(f)$ can be derived. For the case of two-hop system, the ratio of (3.4) and (3.5) is given by,

$$\begin{aligned} \frac{S_s(f)}{S_n(f)} &= \frac{\left| \frac{\sqrt{\gamma_1\gamma_2}}{\sqrt{\gamma_1+\gamma^{\mathrm{rr}}+1}e^{j2\pi f} - \sqrt{\gamma^{\mathrm{rr}}}} \right|^2}{\left| \frac{\sqrt{\gamma_2}}{\sqrt{\gamma_1+\gamma^{\mathrm{rr}}+1}e^{j2\pi f} - \sqrt{\gamma^{\mathrm{rr}}}} \right|^2 + 1} \\ &= \frac{\gamma_1\gamma_2}{\gamma_2 + \left| \sqrt{\gamma_1 + \gamma^{\mathrm{rr}} + 1}e^{j2\pi f} - \sqrt{\gamma^{\mathrm{rr}}} \right|^2} \\ &= \frac{\gamma_1\gamma_2}{\gamma_2 + \gamma_1 + 2\gamma^{\mathrm{rr}} + 1 - 2\sqrt{\gamma^{\mathrm{rr}}\left(\gamma_1 + \gamma^{\mathrm{rr}} + 1\right)} cos(2\pi f)}. \end{aligned} \tag{3.19}$$

Substituting $S_s(f)/S_n(f)$ into (3.3) and simplifying,

$$\gamma_{\text{eq}} = exp\left[\int_{-\frac{1}{2}}^{\frac{1}{2}} \log\left(\frac{\gamma_1\gamma_2+\gamma_2+\gamma_1+2\gamma^{\text{rr}}+1-2\sqrt{\gamma^{\text{rr}}\left(\gamma_1+\gamma^{\text{rr}}+1\right)}cos(2\pi f)}{\gamma_2+\gamma_1+2\gamma^{\text{rr}}+1-2\sqrt{\gamma^{\text{rr}}\left(\gamma_1+\gamma^{\text{rr}}+1\right)}cos(2\pi f)}\right)\,\mathrm{d}f\right]-1. \tag{3.20}$$

With the help of [76], the exponent in (3.20) can be simplified to get,

$$\begin{aligned}\gamma_{\text{eq}} &= \frac{Q_1+\sqrt{Q_1^2-Q_3^3}}{Q_2+\sqrt{Q_2^2-Q_3^3}}-1 &(3.21)\\ &= \frac{\gamma_1\gamma_2+\sqrt{Q_1^2-Q_3^3}-\sqrt{Q_2^2-Q_3^3}}{Q_2+\sqrt{Q_2^2-Q_3^3}}\\ &\geq \frac{\gamma_1\gamma_2}{\gamma_1+\gamma_2+2\gamma^{\text{rr}}+1}, &(3.22)\end{aligned}$$

where $Q_1=\gamma_1\gamma_2+\gamma_2+\gamma_1+2\gamma^{\text{rr}}+1$, $Q_2=\gamma_2+\gamma_1+2\gamma^{\text{rr}}+1$, and $Q_3=-2\sqrt{\gamma^{\text{rr}}\left(\gamma_1+\gamma^{\text{rr}}+1\right)}$. The outage probability $\Pr\left(\gamma_{\text{eq}}\leq\Gamma_T\right)$ is upperbounded by

$$\begin{aligned}\Pr\left(\frac{\gamma_1\gamma_2}{\gamma_1+\gamma_2+2\gamma^{\text{rr}}+1}\leq\Gamma_T\right) &= \Pr\left(\gamma^{\text{rr}}\geq\frac{\gamma_1\gamma_2-\Gamma_T\left(\gamma_1+\gamma_2+1\right)}{2\Gamma_T}\right)\\ &= 1-\Pr\left(\gamma^{\text{rr}}\leq\underbrace{\frac{1}{2\Gamma_T}(\gamma_1(\gamma_2-\Gamma_T)-\Gamma_T(\gamma_2+1))}_{=\psi_2}\right)\\ &= 1-\int\int_{\psi_2\geq 0}\left(1-e^{-\frac{\psi_2}{\Gamma^{\text{rr}}}}\right)\frac{1}{\Gamma_1}e^{-\frac{\gamma_1}{\Gamma_1}}\frac{1}{\Gamma_2}e^{-\frac{\gamma_2}{\Gamma_2}}\,\mathrm{d}\gamma_1\,\mathrm{d}\gamma_2.\end{aligned}$$

We can divide the integration region $\psi_2\geq 0$ with integration limits $\Gamma_T\leq\gamma_2<\infty$ and $\gamma_{\text{lt}}\leq\gamma_1<\infty$, where $\gamma_{\text{lt}}=\Gamma_T(\gamma_2+1)/\left(\gamma_2-\Gamma_T\right)$

$$\begin{aligned}\Pr\left(\frac{\gamma_1\gamma_2}{\gamma_1+\gamma_2+2\gamma^{\text{rr}}+1}\leq\Gamma_T\right) &= 1-\int_{\gamma_2=\Gamma_T}^{\infty}\int_{\gamma_1=\gamma_{\text{lt}}}^{\infty}\left(1-e^{-\frac{\psi_2}{\Gamma^{\text{rr}}}}\right)\frac{1}{\Gamma_1}e^{-\frac{\gamma_1}{\Gamma_1}}\frac{1}{\Gamma_2}e^{-\frac{\gamma_2}{\Gamma_2}}\,\mathrm{d}\gamma_1\,\mathrm{d}\gamma_2\\ &= 1-\int_{\gamma_2=\Gamma_T}^{\infty}\frac{1}{\Gamma_1\Gamma_2}e^{-\frac{\gamma_2}{\Gamma_2}}\,\mathrm{d}\gamma_2\int_{\gamma_1=\gamma_{\text{lt}}}^{\infty}\left(1-e^{-\frac{\psi_2}{\Gamma^{\text{rr}}}}\right)e^{-\frac{\gamma_1}{\Gamma_1}}\,\mathrm{d}\gamma_1.\end{aligned} \tag{3.23}$$

For the purpose of simplification, let us consider the RHS of (3.23),

$$
\begin{aligned}
&1-\int_{\gamma_2=\Gamma_T}^{\infty}\frac{1}{\Gamma_1\Gamma_2}e^{-\frac{\gamma_2}{\Gamma_2}}\,\mathrm{d}\gamma_2\int_{\gamma_1=\gamma_{\mathrm{lt}}}^{\infty}\left(1-e^{-\frac{\psi_2}{\Gamma^{\mathrm{rr}}}}\right)e^{-\frac{\gamma_1}{\Gamma_1}}\,\mathrm{d}\gamma_1\\
&=1-\int_{\gamma_2=\Gamma_T}^{\infty}\frac{1}{\Gamma_1\Gamma_2}e^{-\frac{\gamma_2}{\Gamma_2}}\,\mathrm{d}\gamma_2\left[\int_{\gamma_1=\gamma_{\mathrm{lt}}}^{\infty}e^{-\frac{\gamma_1}{\Gamma_1}}\,\mathrm{d}\gamma_1-\int_{\gamma_1=\gamma_{\mathrm{lt}}}^{\infty}e^{-\left(\frac{\psi_2}{\Gamma^{\mathrm{rr}}}+\frac{\gamma_1}{\Gamma_1}\right)}\,\mathrm{d}\gamma_1\right]\\
&=1+\int_{\gamma_2=\Gamma_T}^{\infty}\frac{1}{\Gamma_1\Gamma_2}e^{-\frac{\gamma_2}{\Gamma_2}}\,\mathrm{d}\gamma_2\left[\Gamma_1e^{-\frac{\gamma_1}{\Gamma_1}}\Big|_{\gamma_1=\gamma_{\mathrm{lt}}}^{\infty}+\frac{1}{-\frac{1}{\Gamma^{\mathrm{rr}}}\left(\frac{\gamma_2-\Gamma_T}{2\Gamma_T}\right)-\frac{1}{\Gamma_1}}e^{-\left(\frac{\psi_2}{\Gamma^{\mathrm{rr}}}+\frac{\gamma_1}{\Gamma_1}\right)}\Big|_{\gamma_1=\gamma_{\mathrm{lt}}}^{\infty}\right]\\
&=1+\int_{\gamma_2=\Gamma_T}^{\infty}\frac{1}{\Gamma_1\Gamma_2}e^{-\frac{\gamma_2}{\Gamma_2}}\,\mathrm{d}\gamma_2\left[-\Gamma_1e^{-\frac{\Gamma_T(\gamma_2+1)}{\Gamma_1(\gamma_2-\Gamma_T)}}+\frac{1}{\frac{1}{\Gamma^{\mathrm{rr}}}\left(\frac{\gamma_2-\Gamma_T}{2\Gamma_T}\right)+\frac{1}{\Gamma_1}}e^{-\frac{\Gamma_T(\gamma_2+1)}{\Gamma_1(\gamma_2-\Gamma_T)}}\right]\\
&=1-\int_{\gamma_2=\Gamma_T}^{\infty}\frac{1}{\Gamma_2}e^{-\frac{\gamma_2}{\Gamma_2}}\,\mathrm{d}\gamma_2\left[\frac{\Gamma_1\left(\gamma_2-\Gamma_T\right)}{\Gamma_1\left(\gamma_2-\Gamma_T\right)+2\Gamma^{\mathrm{rr}}\Gamma_T}e^{-\frac{\Gamma_T(\gamma_2+1)}{\Gamma_1(\gamma_2-\Gamma_T)}}\right]\\
&=1-\int_{z=0}^{\infty}\frac{1}{\Gamma_2}e^{\frac{-\Gamma_T-z}{\Gamma_2}}\left[\frac{\Gamma_1z}{\Gamma_1z+2\Gamma^{\mathrm{rr}}\Gamma_T}e^{-\frac{\Gamma_T(\Gamma_T+z+1)}{\Gamma_1z}}\right]\,\mathrm{d}z\\
&=1-\frac{e^{-\frac{\Gamma_T}{\Gamma_2}}e^{-\frac{\Gamma_T}{\Gamma_1}}}{\Gamma_2}\int_{z=0}^{\infty}e^{-\frac{z}{\Gamma_2}}e^{-\frac{\Gamma_T^2+\Gamma_T}{\Gamma_1z}}\frac{\Gamma_1z}{\Gamma_1z+2\Gamma^{\mathrm{rr}}\Gamma_T}\,\mathrm{d}z,
\end{aligned}
\tag{3.24}
$$

where, $z=\gamma_2-\Gamma_T$. Let us consider two different cases. First, when $2\Gamma^{\mathrm{rr}}\Gamma_T/(\Gamma_1\Gamma_2)\ll 1$ i.e., RSI is relatively moderate, we approximate

$$
\frac{\Gamma_1z}{\Gamma_1z+2\Gamma^{\mathrm{rr}}\Gamma_T}\simeq 1-\frac{2\Gamma^{\mathrm{rr}}\Gamma_T}{\Gamma_1}\frac{1}{z},
\tag{3.25}
$$

Substituting (3.25) into (3.24) and applying [76, Eq. 3.471.9],

$$
\begin{aligned}
\Pr(\gamma_{eq}\leq\Gamma_T)&\lessapprox 1-\frac{e^{-\frac{\Gamma_T}{\Gamma_2}}e^{-\frac{\Gamma_T}{\Gamma_1}}}{\Gamma_2}\int_{z=0}^{\infty}e^{-\frac{z}{\Gamma_2}}e^{-\frac{\Gamma_T^2+\Gamma_T}{\Gamma_1z}}\left(1-\frac{2\Gamma^{\mathrm{rr}}\Gamma_T}{\Gamma_1}\frac{1}{z}\right)\,\mathrm{d}z\\
&\approx 1-e^{\left(-\frac{\Gamma_T}{\Gamma_2}\right)}e^{\left(-\frac{\Gamma_T}{\Gamma_1}\right)}\left[\xi_2K_1(\xi_2)-K_0(\xi_2)\frac{4\Gamma_T\Gamma^{\mathrm{rr}}}{\Gamma_1\Gamma_2}\right].
\end{aligned}
\tag{3.26}
$$

Using small-ξ_2 approximations of $K_1(\xi_2)$ and $K_0(\xi_2)\approxeq -\gamma-\log\frac{\xi_2}{2}$, where, γ is the Euler-Gamma constant, we get,

$$
\Pr(\gamma_{eq}\leq\Gamma_T)\approx 1-e^{-\frac{\Gamma_T}{\Gamma_2}}e^{-\frac{\Gamma_T}{\Gamma_1}}\left(1-\underbrace{\frac{4\Gamma^{\mathrm{rr}}\Gamma_T(-\gamma-\log\frac{\xi_2}{2})}{\Gamma_1\Gamma_2}}_{=L_{eq}}\right).
\tag{3.27}
$$

The above outage probability expression has a form similar to outage probability expression using MF (3.18). However, unlike L_{MF}, the outage performance degradation due to the RSI, denoted by L_{eq}, now decreases as Γ_2 grows. Thus, under the moderate RSI, we can expect that equalizing the RSI leads to more graceful performance degradation.

On the other hand, when RSI is very strong, i.e., $\Gamma_1\Gamma_2/(2\Gamma^{\mathrm{rr}}\Gamma_T) \ll 1$, we have

$$\frac{\Gamma_1 z}{\Gamma_1 z + 2\Gamma^{\mathrm{rr}}\Gamma_T} \simeq \frac{\Gamma_1 z}{2\Gamma^{\mathrm{rr}}\Gamma_T}, \tag{3.28}$$

Substituting (3.28) into (3.24), after some simplifications using [76, Eq. 3.471.9] and $K_2(\xi_2) \approx 2\xi_2^{-2}$, we get,

$$\Pr(\gamma_{eq} \leq \Gamma_T) \lessapprox 1 - \frac{\Gamma_1\Gamma_2}{2\Gamma^{\mathrm{rr}}\Gamma_T} e^{-\frac{\Gamma_T}{\Gamma_1}} e^{-\frac{\Gamma_T}{\Gamma_2}}. \tag{3.29}$$

Since $\Gamma_1\Gamma_2/(2\Gamma^{\mathrm{rr}}\Gamma_T) \ll 1$, the outage probability remains close to one. This is because of the fact that under strong RSI, the relay wastes most of its transmit power to amplify the RSI.

We performed the outage probability analysis considering only a single relay (two-hop system). Now let us consider two relays (three-hop system) between the source and the destination and perform outage probability analysis.

3.3.2 Outage Probability Analysis of Three-hop System

Consider a three-hop system (N=2 relay) as shown in Fig. 3.2. When the relays operate in the full-duplex scheme, equations (2.20) and (2.22) can be used to obtain

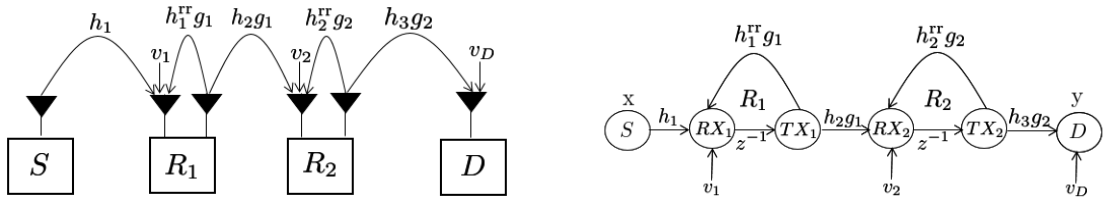

(a) Block diagram (b) Signal-flow graph

Figure 3.2: System Model of Three-hop System

the expressions for $H(z)$ and $H_{\mathrm{n}i}(z)$ as,

$$\begin{aligned} H(z) =& \frac{h_1 z^{-2} \prod_{k=1}^{2} h_{k+1} g_k}{1 + \sum_{k=1}^{2} z^{-k} (-1)^k \sum_{A \in \mathbb{S}_k} \prod_{j \in A} h_j^{\mathrm{rr}} g_j} \\ =& \frac{h_1 h_2 g_1 h_3 g_2 z^{-2}}{1 - \left(h_1^{\mathrm{rr}} g_1 + h_2^{\mathrm{rr}} g_2\right) z^{-1} + h_1^{\mathrm{rr}} g_1 h_2^{\mathrm{rr}} g_2 z^{-2}}, \end{aligned} \tag{3.30}$$

$$H_{\mathrm{n}i}(z) = \frac{z^{-(3-i)} \prod_{k=i}^{2} h_{k+1} g_k}{1 + \sum_{k=1}^{2} z^{-k} (-1)^k \sum_{A \in \mathbb{S}_{k,i}} \prod_{j \in A} h_j^{\mathrm{rr}} g_j}. \tag{3.31}$$

From (3.31), we can obtain expressions for $H_{n1}(z)$ and $H_{n2}(z)$ as

$$H_{n1}(z) = \frac{h_2 g_1 h_3 g_2 z^{-2}}{1 - \left(h_1^{\mathrm{rr}} g_1 + h_2^{\mathrm{rr}} g_2\right) z^{-1} + h_1^{\mathrm{rr}} g_1 h_2^{\mathrm{rr}} g_2 z^{-2}}, H_{n2}(z) = \frac{h_3 g_2 z^{-1}}{1 - h_2^{\mathrm{rr}} g_2 z^{-1}}. \tag{3.32}$$

The overall transform-domain input-output relationship of the system corresponding to both information-bearing signal and noise signal inputs can be obtained from (3.30) and (3.32) as,

$$Y(z) = H(z)X(z) + H_{n1}(z)V_1(z) + H_{n2}(z)V_2(z) + V_D(z). \tag{3.33}$$

By taking inverse z-transform of (3.33), the received symbol at the destination at time n can be determined, which can be used to find the signal and noise components. Using these components, we can calculate the output SNR of the matched filter.

Taking inverse z-transform of (3.33) gives,

$$y[n] = h[n] * x[n] + h_{n1}[n] * v_1[n] + h_{n2}[n] * v_2[n] + v_D[n]. \tag{3.34}$$

The impulse response $h[n]$ can be obtained from (2.29), $h_{n1}[n]$ and $h_{n2}[n]$ can be obtained from (2.34) as,

$$h[n] = h_1 h_2 h_3 g_1 g_2 \left(\frac{m_1^{n-2}}{1 - \frac{m_2}{m_1}} + \frac{m_2^{n-2}}{1 - \frac{m_1}{m_2}} \right) u[n-2], \tag{3.35}$$

$$h_{n1}[n] = h_2 h_3 g_1 g_2 \left(\frac{m_1^{n-2}}{1 - \frac{m_2}{m_1}} + \frac{m_2^{n-2}}{1 - \frac{m_1}{m_2}} \right) u[n-2], \tag{3.36}$$

$$h_{n2}[n] = h_3 g_2 m_2^{n-1} u[n-1], \tag{3.37}$$

where, $m_1 = h_1^{\mathrm{rr}} g_1$ and $m_2 = h_2^{\mathrm{rr}} g_2$. Substituting the expression for $h[n]$, $h_{n1}[n]$ and $h_{n2}[n]$ into (3.34), we obtain

$$\begin{aligned}
y[n] =& h_1 h_2 h_3 g_1 g_2 \left(\frac{m_1^{n-2}}{1 - \frac{m_2}{m_1}} + \frac{m_2^{n-2}}{1 - \frac{m_1}{m_2}} \right) u[n-2] * x[n] \\
&+ h_2 h_3 g_1 g_2 \left(\frac{m_1^{n-2}}{1 - \frac{m_2}{m_1}} + \frac{m_2^{n-2}}{1 - \frac{m_1}{m_2}} \right) u[n-2] * v_1[n] \\
&+ h_3 g_2 m_2^{n-1} u[n-1] * v_2[n] + v_D[n] \\
=& h_1 h_2 h_3 g_1 g_2 \left(\frac{m_1^{n-2}}{1 - \frac{m_2}{m_1}} u[n-2] * x[n] + \frac{m_2^{n-2}}{1 - \frac{m_1}{m_2}} u[n-2] * x[n] \right) \\
&+ h_2 h_3 g_1 g_2 \left(\frac{m_1^{n-2}}{1 - \frac{m_2}{m_1}} u[n-2] * v_1[n] + \frac{m_2^{n-2}}{1 - \frac{m_1}{m_2}} u[n-2] * v_1[n] \right) \\
&+ h_3 g_2 m_2^{n-1} u[n-1] * v_2[n] + v_D[n] \\
=& h_1 h_2 h_3 g_1 g_2 \left(\frac{1}{1 - \frac{m_2}{m_1}} \sum_{k=2}^{\infty} m_1^{k-2} x[n-k] + \frac{1}{1 - \frac{m_1}{m_2}} \sum_{k=2}^{\infty} m_2^{k-2} x[n-k] \right) \\
&+ h_2 h_3 g_1 g_2 \left(\frac{1}{1 - \frac{m_2}{m_1}} \sum_{k=2}^{\infty} m_1^{k-2} v_1[n-k] + \frac{1}{1 - \frac{m_1}{m_2}} \sum_{k=2}^{\infty} m_2^{k-2} v_1[n-k] \right) \\
&+ h_3 g_2 \sum_{k=1}^{\infty} m_2^{k-1} v_2[n-k] + v_D[n].
\end{aligned} \tag{3.38}$$

When the RSI channels h_i^{rr} is not known at the destination, the receiver performs matched filtering (MF) with respect to the strongest tap of the channel, treating all the other taps due to RSI as noise [39]. The effective SNR, γ_{MF}, at the output of the matched filter is given by the ratio of the output signal power to the output noise power.

By noting that $|h_i^{\text{rr}}|^2 g_i^2 < 1$, $|m_1|^2 = |h_1^{\text{rr}}|^2 g_1^2$, $|m_2|^2 = |h_2^{\text{rr}}|^2 g_2^2$, $g_1^2 = 1/(\sigma^2(\gamma_1 + \gamma_1^{\text{rr}} + 1))$ and $g_2^2 = 1/(\sigma^2(\gamma_2 + \gamma_2^{\text{rr}} + 1))$, signal power can be determined from (3.38) as,

$$\text{output signal power} = |h_1|^2|h_2|^2|h_3|^2 g_1^2 g_2^2. \tag{3.39}$$

Similarly, noise power can be determined from (3.38) as,

$$\begin{aligned}
&\text{output noise power} = \\
&|h_1|^2|h_2|^2|h_3|^2 g_1^2 g_2^2 \left(\frac{|m_1|^2}{|m_1|^2 - |m_2|^2} \frac{|m_1|^2}{1 - |m_1|^2} + \frac{|m_2|^2}{|m_2|^2 - |m_1|^2} \frac{|m_2|^2}{1 - |m_2|^2} \right) \\
&+ \sigma^2 |h_2|^2|h_3|^2 g_1^2 g_2^2 \left(\frac{|m_1|^2}{|m_1|^2 - |m_2|^2} \frac{1}{1 - |m_1|^2} + \frac{|m_2|^2}{|m_2|^2 - |m_1|^2} \frac{1}{1 - |m_2|^2} \right) \\
&+ \left(\frac{|h_3|^2 g_2^2}{1 - |m_2|^2} + 1 \right) \sigma^2.
\end{aligned} \tag{3.40}$$

Taking ratio of (3.39) and (3.40), after rearranging some terms, we get the expression for effective output SNR of the MF to be,

$$\begin{aligned}
\gamma_{\text{MF}} &= \frac{|h_1|^2|h_2|^2|h_3|^2 g_1^2 g_2^2}{\frac{|h_2|^2|h_3|^2 g_1^2 g_2^2}{(|m_1|^2 - |m_2|^2)} \left(\frac{|h_1|^2|m_1|^4}{(1-|m_1|^2)} - \frac{|h_1|^2|m_2|^4}{(1-|m_2|^2)} + \frac{\sigma^2|m_1|^2}{1-|m_1|^2} - \frac{\sigma^2|m_2|^2}{1-|m_2|^2} \right) + \left(\frac{|h_3|^2 g_2^2}{1-|m_2|^2} + 1 \right) \sigma^2} \\
&= \frac{1}{\frac{1}{(|m_1|^2 - |m_2|^2)\gamma_1} \left(\frac{\gamma_1|m_1|^4 + |m_1|^2}{1-|m_1|^2} - \frac{\gamma_1|m_2|^4 + |m_2|^2}{1-|m_2|^2} \right) + \frac{\gamma_1 + \gamma_1^{\text{rr}} + 1}{\gamma_1\gamma_2(1-|m_2|^2)} + \frac{(\gamma_1 + \gamma_1^{\text{rr}} + 1)(\gamma_2 + \gamma_2^{\text{rr}} + 1)}{\gamma_1\gamma_2\gamma_3}}.
\end{aligned} \tag{3.41}$$

Though (3.41) is for the three-hop case only, but it can be extended to other cases with multiple hops by following same derivation steps as above. Since MF treats RSI as noise, it does not use the useful information present in RSI. On the other hand, equalizers can be used at the destination which takes advantage of the useful information in RSI.

We consider that the frequency-selective channel introduced by RSI is equalized by employing different types of equalizers at the destination. We can see that the output SNR expression of the equalizers (3.1),(3.2) and(3.3), contains the ratio $S_s(f)/S_n(f)$ which can be determined from (3.30) and (3.31) by noting that $S_s(f) = |H(e^{j2\pi f})|^2$ and $S_{n_i}(f) = |H_{\mathrm{n}i}(e^{j2\pi f})|^2$. Using (3.6), one can obtain the ratio $S_s(f)/S_n(f)$ as

$$\begin{aligned}\frac{S_s(f)}{S_n(f)} &= \frac{\left|\frac{e^{-j4\pi f}\frac{\sqrt{\gamma_1\gamma_2\gamma_3}}{PQ}}{1-\left(\frac{\sqrt{\gamma_1^{\mathrm{rr}}}}{P}+\frac{\sqrt{\gamma_2^{\mathrm{rr}}}}{Q}\right)e^{-j2\pi f}+\frac{\sqrt{\gamma_1^{\mathrm{rr}}\gamma_2^{\mathrm{rr}}}}{PQ}e^{-j4\pi f}}\right|^2}{\left|\frac{e^{-j4\pi f}\frac{\sqrt{\gamma_2\gamma_3}}{PQ}}{1-\left(\frac{\sqrt{\gamma_1^{\mathrm{rr}}}}{P}+\frac{\sqrt{\gamma_2^{\mathrm{rr}}}}{Q}\right)e^{-j2\pi f}+\frac{\sqrt{\gamma_1^{\mathrm{rr}}\gamma_2^{\mathrm{rr}}}}{PQ}e^{-j4\pi f}}\right|^2+\left|\frac{e^{-j2\pi f}\frac{\sqrt{\gamma_3}}{Q}}{1-\frac{\sqrt{\gamma_2^{\mathrm{rr}}}}{Q}e^{-j2\pi f}}\right|^2+1} \\ &= \frac{\gamma_1}{1+\underbrace{\left[\left|\frac{e^{-j2\pi f}\frac{\sqrt{\gamma_3}}{Q}}{1-\frac{\sqrt{\gamma_2^{\mathrm{rr}}}}{Q}e^{-j2\pi f}}\right|^2+1\right]}_{A_{eq}}\underbrace{\left|\frac{1-\left(\frac{\sqrt{\gamma_1^{\mathrm{rr}}}}{P}+\frac{\sqrt{\gamma_2^{\mathrm{rr}}}}{Q}\right)e^{-j2\pi f}+\frac{\sqrt{\gamma_1^{\mathrm{rr}}\gamma_2^{\mathrm{rr}}}}{PQ}e^{-j4\pi f}}{e^{-j4\pi f}\frac{\sqrt{\gamma_2\gamma_3}}{PQ}}\right|^2}_{B_{eq}}},\end{aligned} \tag{3.42}$$

where, $P = \sqrt{\gamma_1 + \gamma_1^{\mathrm{rr}} + 1}$ and $Q = \sqrt{\gamma_2 + \gamma_2^{\mathrm{rr}} + 1}$. Let, $R = \sqrt{\gamma_1^{\mathrm{rr}}}Q + \sqrt{\gamma_2^{\mathrm{rr}}}P$, we consider A_{eq} and B_{eq} separately to simplify them. Consider A_{eq} as in (3.42)

$$\begin{aligned}A_{eq} &= \left|\frac{e^{-j2\pi f}\frac{\sqrt{\gamma_3}}{Q}}{1-\frac{\sqrt{\gamma_2^{\mathrm{rr}}}}{Q}e^{-j2\pi f}}\right|^2+1 \\ &= \left|\frac{\sqrt{\gamma_3}}{Qe^{j2\pi f}-\sqrt{\gamma_2^{\mathrm{rr}}}}\right|^2+1 \\ &= \left|\frac{\sqrt{\gamma_3}}{Q\cos(2\pi f)-\sqrt{\gamma_2^{\mathrm{rr}}}+iQ\sin(2\pi f)}\right|^2+1.\end{aligned} \tag{3.43}$$

For simplification, let us multiply and divide the first term in (3.43) by $Q\cos(2\pi f)-$

$\sqrt{\gamma_2^{\text{rr}}} - iQ\sin(2\pi f)$,

$$\begin{aligned}
A_{eq} &= \left| \frac{\sqrt{\gamma_3}}{Q\cos(2\pi f) - \sqrt{\gamma_2^{\text{rr}}} + iQ\sin(2\pi f)} \times \frac{Q\cos(2\pi f) - \sqrt{\gamma_2^{\text{rr}}} - iQ\sin(2\pi f)}{Q\cos(2\pi f) - \sqrt{\gamma_2^{\text{rr}}} - iQ\sin(2\pi f)} \right|^2 + 1 \\
&= \frac{\gamma_3 \left[\left(Q\cos(2\pi f) - \sqrt{\gamma_2^{\text{rr}}}\right)^2 + \left(Q\sin(2\pi f)\right)^2 \right]}{\left[\left(Q\cos(2\pi f) - \sqrt{\gamma_2^{\text{rr}}}\right)^2 + \left(Q\sin(2\pi f)\right)^2 \right]^2} + 1 \\
&= \frac{\gamma_3}{\gamma_2 + 2\gamma_2^{\text{rr}} + 1 - 2Q\sqrt{\gamma_2^{\text{rr}}}\cos(2\pi f)} + 1 \\
&= \frac{\gamma_3 + \gamma_2 + 2\gamma_2^{\text{rr}} + 1 - 2Q\sqrt{\gamma_2^{\text{rr}}}\cos(2\pi f)}{\gamma_2 + 2\gamma_2^{\text{rr}} + 1 - 2Q\sqrt{\gamma_2^{\text{rr}}}\cos(2\pi f)}.
\end{aligned} \tag{3.44}$$

Consider B_{eq} as in (3.42)

$$\begin{aligned}
B_{eq} &= \left| \frac{1 - \left(\frac{\sqrt{\gamma_1^{\text{rr}}}}{P} + \frac{\sqrt{\gamma_2^{\text{rr}}}}{Q} \right) e^{-j2\pi f} + \frac{\sqrt{\gamma_1^{\text{rr}}\gamma_2^{\text{rr}}}}{PQ} e^{-j4\pi f}}{e^{-j4\pi f} \frac{\sqrt{\gamma_2\gamma_3}}{PQ}} \right|^2 \\
&= \frac{1}{\gamma_2\gamma_3} \left| PQe^{j4\pi f} - e^{j2\pi f} \underbrace{\left(\sqrt{\gamma_1^{\text{rr}}}Q + \sqrt{\gamma_2^{\text{rr}}}P \right)}_{R} + \sqrt{\gamma_1^{\text{rr}}\gamma_2^{\text{rr}}} \right|^2 \\
&= \frac{1}{\gamma_2\gamma_3} \left[PQ\cos(4\pi f) - R\cos(2\pi f) + \sqrt{\gamma_1^{\text{rr}}\gamma_2^{\text{rr}}} \right]^2 + \left[PQ\sin(4\pi f) - R\sin(2\pi f) \right]^2.
\end{aligned} \tag{3.45}$$

After some simplification, we get

$$\begin{aligned}
B_{eq} = \frac{1}{\gamma_2\gamma_3} &\left[(PQ)^2 + R^2 - 2R\left(PQ + \sqrt{\gamma_1^{\text{rr}}\gamma_2^{\text{rr}}} \right)\cos(2\pi f) \right] \\
&+ \frac{1}{\gamma_2\gamma_3} \left[2PQ\sqrt{\gamma_1^{\text{rr}}\gamma_2^{\text{rr}}}\cos(4\pi f) + \gamma_1^{\text{rr}}\gamma_2^{\text{rr}} \right].
\end{aligned} \tag{3.46}$$

Substituting (3.44) into (3.42),

$$\frac{S_s(f)}{S_n(f)} = \frac{\gamma_1}{1 + \left(\frac{\gamma_2 + \gamma_3 + 2\gamma_2^{\text{rr}} + 1 - 2\sqrt{\gamma_2^{\text{rr}}}Q\cos(2\pi f)}{\gamma_2 + 2\gamma_2^{\text{rr}} + 1 - 2\sqrt{\gamma_2^{\text{rr}}}Q\cos(2\pi f)} \right) B_{eq}}, \tag{3.47}$$

where, B_{eq} is as given in (3.46). Substituting (3.47) into (3.1), (3.2) and (3.3), we can get the exact output SNR expression of the respective equalizers.

One can see that for a multi-hop network after the substitution of (3.47) into (3.1), (3.2) and (3.3), the complexity of solving the integrals increases as the number of relays in the network increases. Therefore, for simplicity one can assume that there will be perfect self-interference cancellation at one of the relays and it is seen that for the case of a three-hop system, the integral in (3.3) can be solved easily to get a closed-form upper bound on output SNR of MMSE-DFE.

Perfect Self-interference Cancellation at R_1:

Considering a full-duplex amplify-and-forward three-hop network with MMSE-DFE at the destination, by assuming that there will be perfect self-interference cancellation at R_1, we derive an upper bound on the output SNR.

Substituting $\gamma_1^{\mathrm{rr}} = 0$ into (3.46),

$$B'_{eq} = \frac{1}{\gamma_2\gamma_3}\left[(\gamma_1+1)\,Q^2 + \gamma_2^{\mathrm{rr}}\,(\gamma_1+1) - 2Q\,(\gamma_1+1)\,\sqrt{\gamma_2^{\mathrm{rr}}}\cos(2\pi f)\right]. \tag{3.48}$$

Substituting (3.48) into (3.47) in the place of B_{eq} and subsequently into (3.3), we obtain

$$\gamma_{\mathrm{eq}} \leq -1 + \exp\left(\int_{-\frac{1}{2}}^{\frac{1}{2}} \log\left(1 + \frac{\gamma_1}{1 + A_{eq}B'_{eq}}\right)\,\mathrm{d}f\right). \tag{3.49}$$

The equation (3.49) can be rewritten as given in (3.50) by defining, $U = \gamma_2\gamma_3 + (\gamma_1+1)\,(\gamma_2+\gamma_3+2\gamma_2^{\mathrm{rr}}+1)$. Using [76, Eq. 4.224.9], (3.50) can be simplified to obtain upper bound on the output SNR as given in (3.51).

Perfect Self-interference Cancellation at R_2:

Considering a full-duplex amplify-and-forward three-hop network with MMSE-DFE at the destination, by assuming that there will be perfect self-interference cancellation at R_2, we derive an upper bound on the output SNR.

$$\gamma_{\text{eq}} \leq -1 + \exp\left(\int_{-\frac{1}{2}}^{\frac{1}{2}} \log\left(\gamma_1\gamma_2\gamma_3 + U - 2Q\left(\gamma_1+1\right)\sqrt{\gamma_2^{\text{rr}}}\cos(2\pi f)\right)\,\mathrm{d}f\right)$$
$$\exp\left(-\int_{-\frac{1}{2}}^{\frac{1}{2}} \log\left(U - 2Q\left(\gamma_1+1\right)\sqrt{\gamma_2^{\text{rr}}}\cos(2\pi f)\right)\,\mathrm{d}f\right). \tag{3.50}$$

$$\gamma_{\text{eq}} \leq -1 + \frac{\gamma_1\gamma_2\gamma_3+\gamma_2\gamma_3+(\gamma_1+1)(\gamma_2+\gamma_3+2\gamma_2^{\text{rr}}+1)+\sqrt{\left[\gamma_1\gamma_2\gamma_3+\gamma_2\gamma_3+(\gamma_1+1)\left(\gamma_2+\gamma_3+2\gamma_2^{\text{rr}}+1\right)\right]^2-4\gamma_2^{\text{rr}}Q^2(\gamma_1+1)^2}}{\gamma_2\gamma_3+(\gamma_1+1)\left(\gamma_2+\gamma_3+2\gamma_2^{\text{rr}}+1\right)+\sqrt{\left[\gamma_2\gamma_3+(\gamma_1+1)\left(\gamma_2+\gamma_3+2\gamma_2^{\text{rr}}+1\right)\right]^2-4\gamma_2^{\text{rr}}Q^2(\gamma_1+1)^2}}. \tag{3.51}$$

Substituting $\gamma_2^{\text{rr}} = 0$ into (3.44) and (3.46),

$$A'_{eq} = \frac{\gamma_3+\gamma_2+1}{\gamma_2+1}, \tag{3.52}$$

$$B''_{eq} = \frac{1}{\gamma_2\gamma_3}\left[\left(\gamma_2+1\right)P^2 + \gamma_1^{\text{rr}}\left(\gamma_2+1\right) - 2P\left(\gamma_2+1\right)\sqrt{\gamma_1^{\text{rr}}}\cos(2\pi f)\right]. \tag{3.53}$$

Substituting (3.52) and (3.53) into (3.47) in the place of A_{eq} and B_{eq} respectively and subsequently into (3.3), we obtain

$$\begin{aligned}\gamma_{\text{eq}} &\leq -1 + \exp\left(\int_{-\frac{1}{2}}^{\frac{1}{2}} \log\left(1 + \frac{\gamma_1}{1+A'_{eq}B''_{eq}}\right)\,\mathrm{d}f\right)\\ &= 1 + \exp\left(\int_{-\frac{1}{2}}^{\frac{1}{2}} \log\left(1 + \frac{\gamma_1\gamma_2\gamma_3}{\gamma_2\gamma_3+\left(\gamma_3+\gamma_2+1\right)\left(P^2+\gamma_1^{\text{rr}}-2P\sqrt{\gamma_1^{\text{rr}}}\cos(2\pi f)\right)}\right)\,\mathrm{d}f\right).\end{aligned} \tag{3.54}$$

Using [76, Eq. 4.224.9], (3.54) can be simplified to obtain upper bound on the output SNR (3.55).

$$\gamma_{\text{eq}} \leq -1 + \frac{\gamma_1\gamma_2\gamma_3+\gamma_2\gamma_3+\left(P^2+\gamma_1^{\text{rr}}\right)(\gamma_2+\gamma_3+1)+\sqrt{\left[\gamma_1\gamma_2\gamma_3+\gamma_2\gamma_3+\left(P^2+\gamma_1^{\text{rr}}\right)(\gamma_2+\gamma_3+1)\right]^2-4\gamma_1^{\text{rr}}P^2(\gamma_2+\gamma_3+1)^2}}{\gamma_2\gamma_3+\left(P^2+\gamma_1^{\text{rr}}\right)(\gamma_2+\gamma_3+1)+\sqrt{\left[\gamma_2\gamma_3+\left(P^2+\gamma_1^{\text{rr}}\right)(\gamma_2+\gamma_3+1)\right]^2-4\gamma_1^{\text{rr}}P^2(\gamma_2+\gamma_3+1)^2}}. \tag{3.55}$$

Using (3.51) and (3.55), we can calculate a bound on the outage probability of the end-to-end network using Monte Carlo simulations. The bounds on outage probability obtained are lower bounds since the outage probability decreases as the output SNR of the MMSE-DFE increases due to perfect self-interference cancellation. The

benefit of these bounds compared to exact outage calculation is that they require less simulation time as compared to solving the integral in (3.3) to get the exact value. In the simulations we see that the bound in (3.55) is tighter. This is because even though there is perfect self-interference cancellation at R_2, RSI from R_1 propagates to subsequent relays.

When the relays operate in the half-duplex scheme, the output SNR of the end-to-end system is given by [78, Eq. 2],

$$\gamma_{\text{out}} = \left(\prod_{i=1}^{N+1} \left(1 + \frac{1}{\gamma_i} \right) - 1 \right)^{-1} , \tag{3.56}$$

where, γ_{i} is the SNR of the i^{th} hop. We consider that the end-to-end link is in outage when the output SNR, γ_{out}, is below a threshold Γ_{T}, which is given by $\Gamma_T = 2^{2R_T} - 1$.

3.4 Outage Probability Analysis of Multi-hop Amplify-and-forward Full-duplex Relaying Systems with Frequency-selective Fading Channels

We now consider frequency-selective fading on each link between consecutive relays as shown in Fig. 3.3 and Fig. 3.4 so that those channels are now functions of z represented by a degree $\nu - 1$ polynomial representing a length ν channel. We can

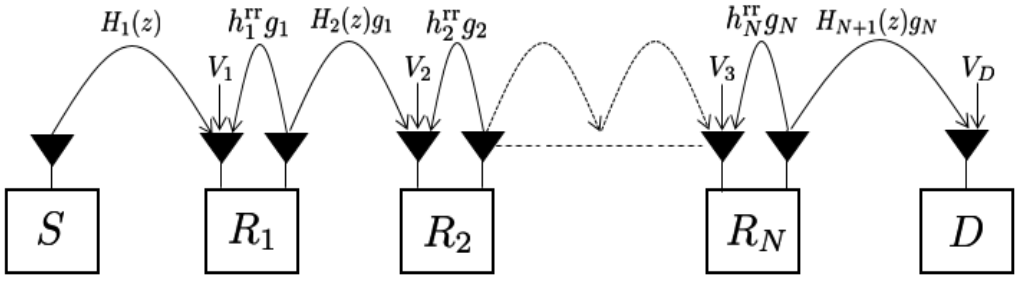

Figure 3.3: System Model with $(N+1)$ hops and Frequency-selective Fading Channels

still use (2.20) and (2.22) with the substitution $h_i \to H_i(z)$, where $H_i(z)$ is given by

$$H_i(z) = \sum_{l=0}^{\nu-1} h_i[l] z^{-l} \ . \tag{3.57}$$

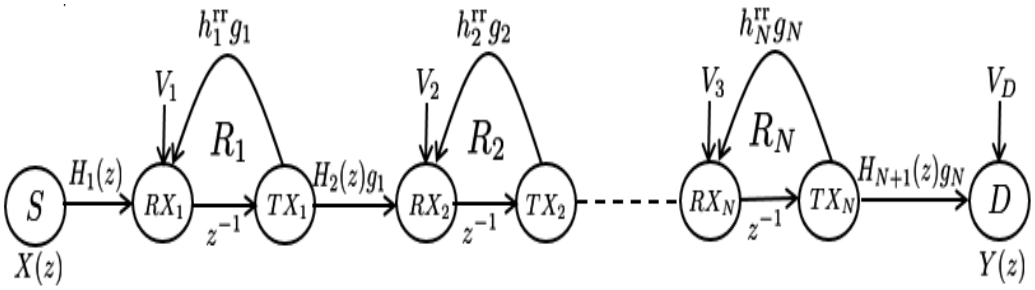

Figure 3.4: Signal-flow Graph with Frequency-selective Fading Channels

This yields,

$$H(z) = \frac{H_1(z)z^{-N}\prod_{k=1}^{N} H_{k+1}(z)g_k}{1+\sum_{k=1}^{N} z^{-k}(-1)^k \sum_{A\in\mathbb{S}_k}\prod_{j\in A} h_j^{\mathrm{rr}} g_j} \quad , \tag{3.58}$$

$$H_{\mathrm{n}i}(z) = \frac{z^{-(N-i+1)}\prod_{k=i}^{N} H_{k+1}(z)g_k}{1+\sum_{k=1}^{N} z^{-k}(-1)^k \sum_{A\in\mathbb{S}_{k,i}}\prod_{j\in A} h_j^{\mathrm{rr}} g_j} \quad . \tag{3.59}$$

We define mean SNR of the hops for the case of frequency-selective channels as,

$$\Gamma_i = E\left[\frac{\sum_{l=0}^{\nu-1}|h_i[l]|^2}{\sigma_v^2}\right] = \frac{\sigma_h^2}{\sigma_v^2}\,, \tag{3.60}$$

where, the last equality is because the impulse response co-efficients $h_i[l]$ are assumed to be complex Gaussian with zero mean and variance σ_h^2/ν.

By assuming that the relays transmit at normalized average power of unity and the relays have the control over their amplification factor g_i, the amplification factor at the relays when the relay channels undergo frequency-selective fading is given by (3.61). In contrast, one can assume that the relays perform filtering operation and thus g_i can be functions of z. We have assumed that the relays do not perform filtering for simplicity so that,

$$g_i = \left(\sum_{l=0}^{\nu-1}|h_i[l]|^2 + |h_i^{\mathrm{rr}}|^2 + \sigma_v^2\right)^{-\frac{1}{2}} . \tag{3.61}$$

Substituting (3.58) and (3.59) into (3.10) one can obtain the input-output relation of multi-hop system with frequency-selective fading channels. As an example, for the case of a three-hop network with 2 taps, using (3.61), equations in (3.58) and (3.59) can be modified to get,

$$H(z)=\sigma_v\frac{\frac{\left(\sqrt{\gamma_{a_1}}+\sqrt{\gamma_{b_1}}z^{-1}\right)\left(\sqrt{\gamma_{a_2}}+\sqrt{\gamma_{b_2}}z^{-1}\right)\left(\sqrt{\gamma_{a_3}}+\sqrt{\gamma_{b_3}}z^{-1}\right)}{\sqrt{\left(\gamma_1+\gamma_1^{\mathrm{rr}}+1\right)\left(\gamma_2+\gamma_2^{\mathrm{rr}}+1\right)}}z^{-2}}{1-\left(\sqrt{\frac{\gamma_1^{\mathrm{rr}}}{\gamma_1+\gamma_1^{\mathrm{rr}}+1}}+\sqrt{\frac{\gamma_{2\mathrm{rr}}}{\gamma_2+\gamma_2^{\mathrm{rr}}+1}}\right)z^{-1}+\sqrt{\frac{\gamma_1^{\mathrm{rr}}\gamma_2^{\mathrm{rr}}}{\left(\gamma_1+\gamma_1^{\mathrm{rr}}+1\right)\left(\gamma_2+\gamma_2^{\mathrm{rr}}+1\right)}}z^{-2}}, \tag{3.62}$$

$$H_{\mathrm{n1}}(z)=H(z)/H_1(z), \tag{3.63}$$

$$H_{\mathrm{n2}}=\left(\sqrt{\gamma_{a_3}}+\sqrt{\gamma_{b_3}}z^{-1}\right)z^{-1}/\left(\sqrt{\gamma_2+\gamma_2^{\mathrm{rr}}+1}-\sqrt{\gamma_2^{\mathrm{rr}}}z^{-1}\right). \tag{3.64}$$

One can obtain the ratio $S_s(f)/S_n(f)$ using (3.62), (3.63) and (3.64) as discussed in the previous section and then substituting the resulting ratio into (3.1),(3.2) and (3.3), one can obtain the output SNR of the equalizers. This SNR can be used to simulate the outage performance of the three-hop network with the relay channels undergoing frequency-selective fading.

3.5 Simulation Results

In this section, we present the outage performance of a two-hop full-duplex system and a three-hop full-duplex system based on the output SNR of the equalizers and MF at the destination. Also, we present simulation results for outage probability comparison of half-duplex relaying and full-duplex relaying. For the case of three-hop full-duplex system, we present the simulation results for the outage probability bounds and we also discuss the effects of number of relays on the outage probability in a multi-hop full-duplex amplify-and-forward relaying system.

Fig. 3.5 shows the outage probability of a two-hop system with different amplify-and-forward schemes for $R_T = 1$ bps/Hz with varying the RSI power. We can see that

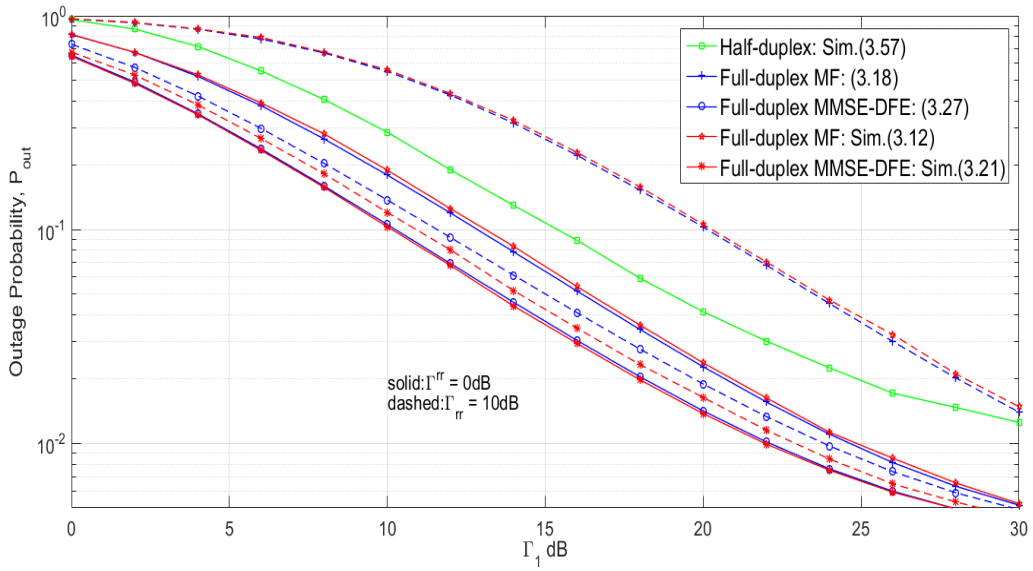

Figure 3.5: Outage Probability of a Two-hop System with Different Amplify-and-forward Relaying (Γ^{rr} =0, 10 dB, R_T=1 bps/Hz, Γ_2=25 dB)

if the relays operate in full-duplex scheme with the matched filtering is quite vulnerable to the RSI, which can be seen that when Γ^{rr}=10dB this scheme is outperformed by half-duplex scheme. In contrast, equalizing the channel by using MMSE-DFE is shown to make full duplex scheme more robust to RSI.

Fig. 3.6 shows the minimum Γ_1 required to achieve 5% outage probability of a two-hop system with R_T=2 bps/Hz. When the RSI is strong, one can see that by considering that the RSI has some useful information about transmitted symbols and not as noise, full-duplex relaying scheme provides robust performance. In contrast, when the RSI is weak, performance loss due to treating the RSI as noise is small.

Fig. 3.7 presents an outage comparison between half-duplex relaying and full-duplex relaying with MF at the destination, or specific equalizers at the destination. Full-duplex relaying with equalizers is seen to outperform half-duplex relaying for $R_T > 1$bps/Hz even with strong RSI. Full-duplex relaying with MF at the destination also outperforms half-duplex relaying for target rates $R_T \geq 3.5$bps/Hz under strong RSI. As Γ^{rr} decreases, the crossover point of half-duplex relaying and full-duplex

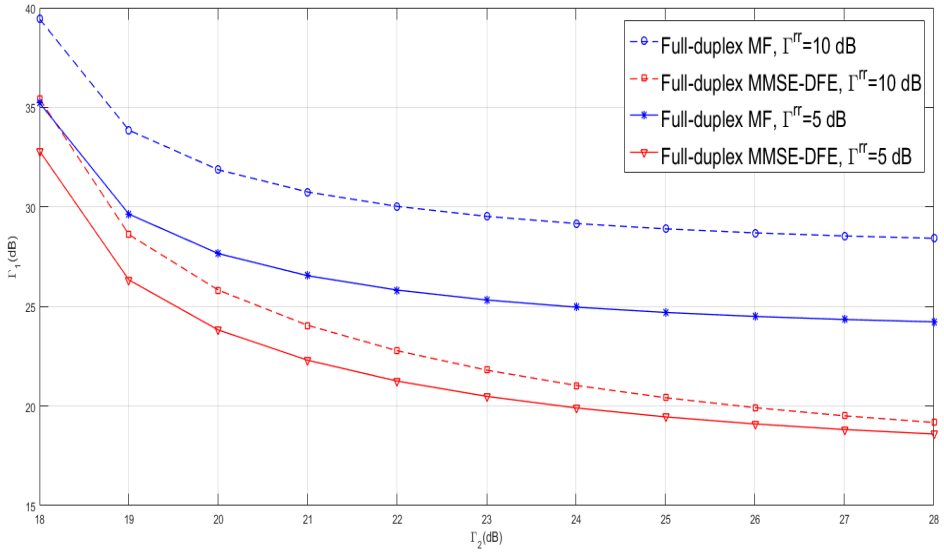

Figure 3.6: Minimum Γ_1 Required to Achieve 5% Outage Probability of a Two-hop System with R_T=2 bps/Hz.

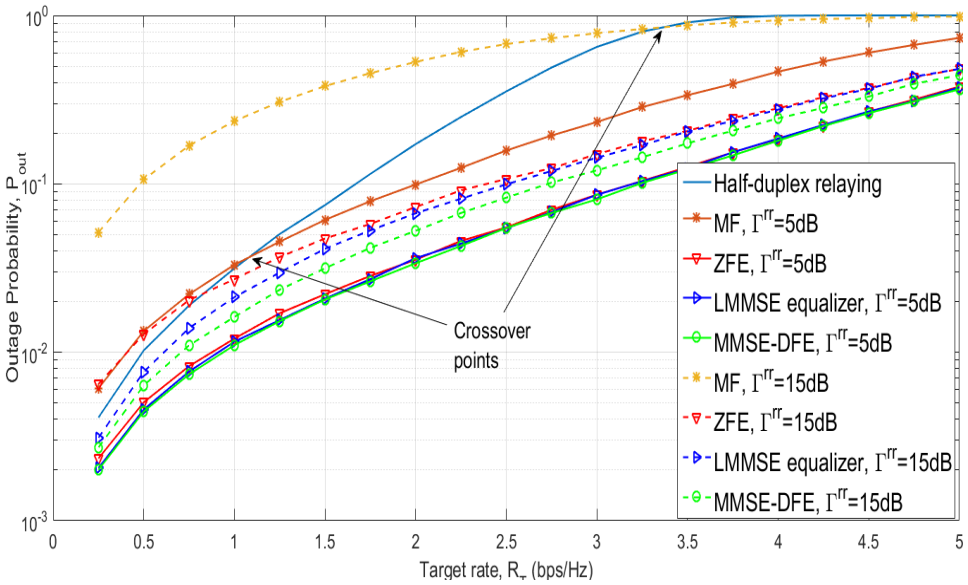

Figure 3.7: Outage Probability vs Rate (R_T) of Three-hop Half-duplex and Full-duplex Networks with all the Links having Flat Fading ($R_T = 1$ bps/Hz, $\Gamma_1 = \Gamma_2 = \Gamma_3 = 25$ dB)

relaying with MF curves is observed to shift towards the lower outage probability region in Fig. 3.7. At low RSI (Γ^{rr}=5dB), for sufficiently high target rates, both full-duplex relaying with equalizers and MF outperform half-duplex relaying with

different crossover points.

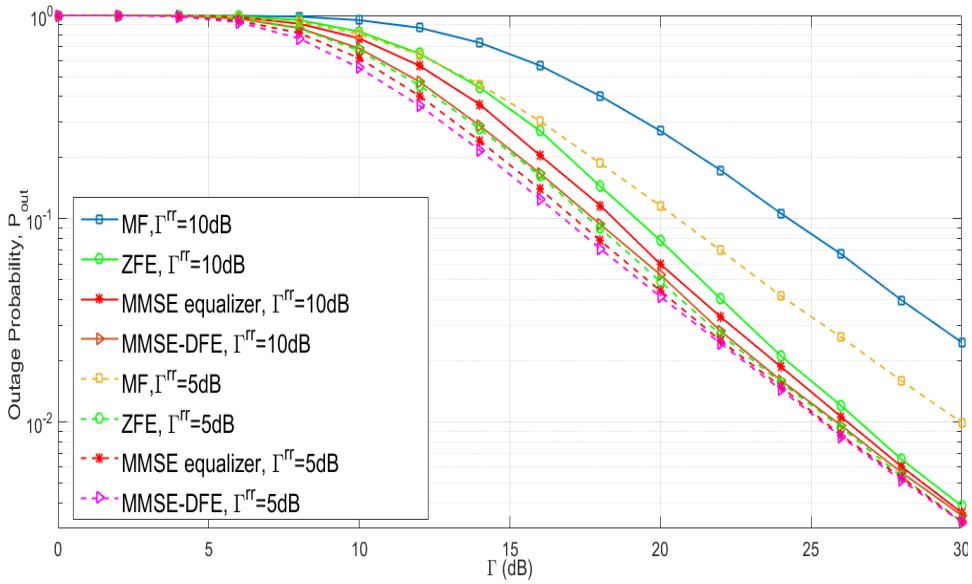

Figure 3.8: Outage Probability of a Three-hop System when the Destination Employs Various Types of Equalizers with all the Links having Flat Fading ($\Gamma_1^{\text{rr}} = \Gamma_2^{\text{rr}} = \Gamma^{\text{rr}}$, $R_T = 1$ bps/Hz, $\Gamma_1 = \Gamma_2 = \Gamma_3 = \Gamma$)

Fig. 3.8 shows the outage performance of the system when the destination employs MF and different types of equalizers to equalize the effective channel. It is seen that employing MMSE-DFE at the destination gives a better outage probability performance compared to employing linear MMSE equalizer or zero-forcing equalizer or MF for the same value of Γ. Since MF considers RSI as noise, which is in contrast with equalizers, outage performance of MF is worse in comparison. We also see that as Γ^{rr} increases, P_{out} also increases which is due to the decrease in end-to-end SNR.

Fig. 3.9 shows the comparison of the bounds on the outage probability of a three-hop system when either $\gamma_1^{\text{rr}} = 0$ or $\gamma_2^{\text{rr}} = 0$. When $\gamma_2^{\text{rr}} = 0$, RSI is amplified twice before the signal is received at the destination. Once, in R_1 due to the presence of γ_1^{rr} and a second-time in R_2 due to RSI forwarded from R_1. In contrast, when $\gamma_1^{\text{rr}} = 0$ RSI is amplified only in R_2. Due to this effect of amplification of the RSI signal at the relays, it is seen that achieving perfect self-interference cancellation at

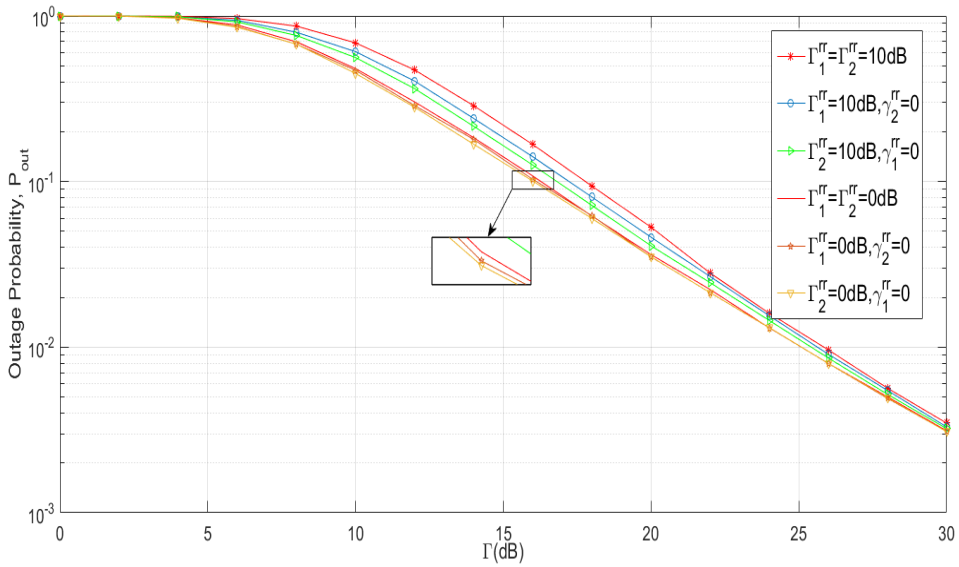

Figure 3.9: Comparison of Lower Bound on the Outage Probability of a Three-hop System when the Destination uses MMSE-DFE with all the Links having Flat Fading ($R_T = 1$ bps/Hz, $\Gamma_2 = \Gamma_3 = 20$ dB)

the relays which are near to the transmitter can perform better in terms of achieving lower outage probability. The bound obtained when $\gamma_2^{\text{rr}} = 0$ is tighter since the exact outage probability curve is the worst case when RSI is present at all the relays.

Fig. 3.10 shows the outage probability of the N=3 hop system with all the links having frequency-selective fading for different equalizers. It is seen that MMSE-DFE outperforms the LMMSE equalizer and ZFE in frequency-selective channels as well as frequency-flat channels ($\nu = 1$). The LMMSE equalizer and MMSE-DFE in frequency-selective channels takes advantage of diversity, which can be seen in the increased slope of their respective outage curves.

Fig. 3.11 shows the effect of number of relays on the outage probability when the number of relays between S and D is increased and the end-to-end channel is equalized by MMSE-DFE at the destination. We consider a fixed average SNR between consecutive relays, which corresponds to increased coverage but degradation of performance with increased number of relays, due to noise amplification. It is seen

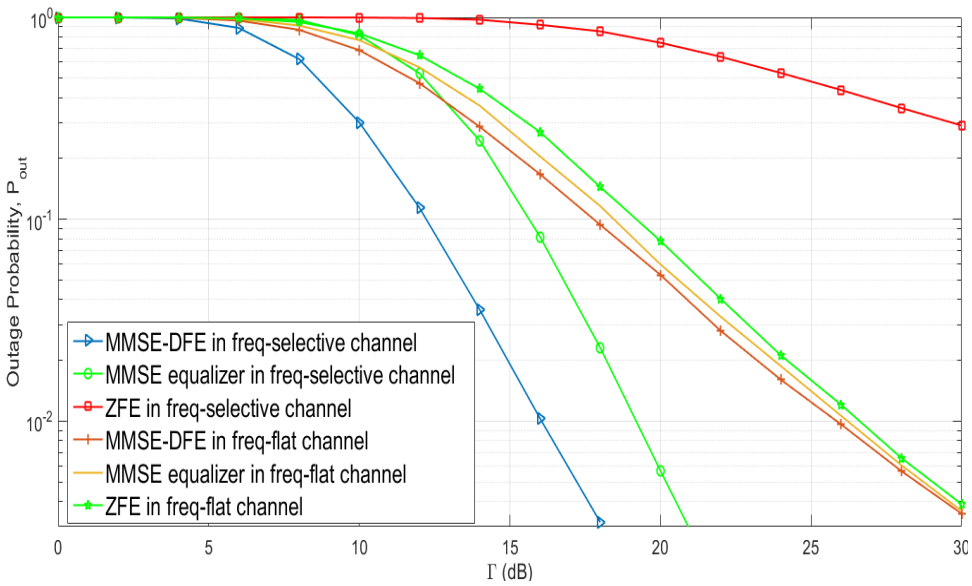

Figure 3.10: Outage Probability of a Three-hop System with all the Relay Links having Frequency-selective Fading ($\nu = 2, \Gamma_1^{\text{rr}} = \Gamma_2^{\text{rr}} = 10$ dB, $R_T = 1$ bps/Hz, $\Gamma_1 = \Gamma_2 = \Gamma_3 = \Gamma$ (dB))

that especially for large average SNR Γ, there is a rapid degradation in outage when the number of relays is increased beyond N=5 or N=6. This indicates that there is a limit to increasing coverage by increasing N in full-duplex amplify-and-forward multi-hop systems.

3.6 Conclusions

In this chapter, we performed the outage probability analysis of a multi-hop full-duplex amplify-and-forward relaying system consider matched filtering and different types of equalizers at the destination. For the case of a two-hop system, we derived the bounds on the outage probability. For the case of a three-hop system, we derived the exact output SNR of matched filter and also we derived the upper bounds on the output SNR of MMSE-DFE. Using the derived SNR expressions we performed the outage probability analysis of the system. In the simulation we showed that MF suffers more from RSI compared to equalizers and among the different types of

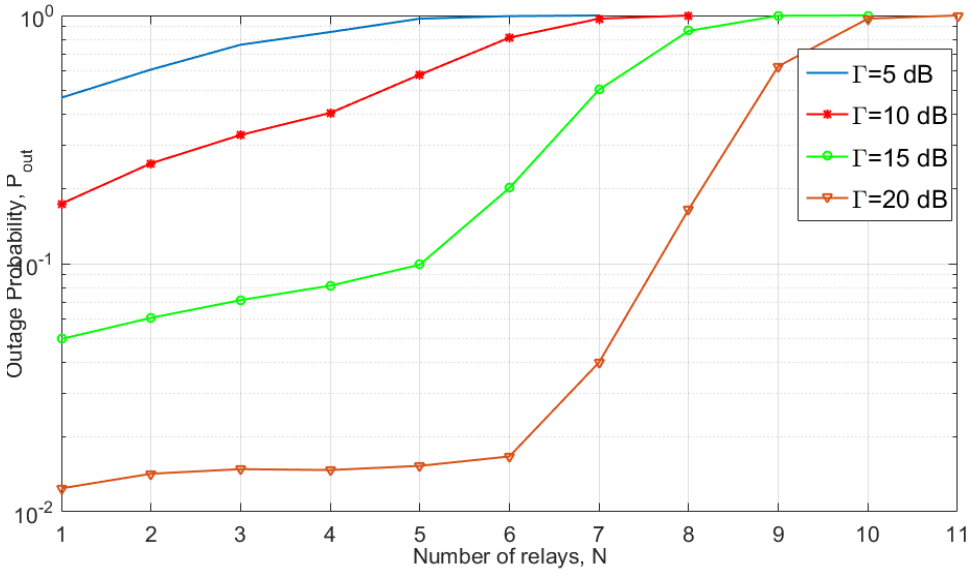

Figure 3.11: Effect of Number of Relays on the Outage Probability with all the Relay Links having Frequency Flat Fading ($\Gamma_1^{\text{rr}} = \Gamma_2^{\text{rr}} = \cdots = \Gamma_N^{\text{rr}} = 0$ dB, $R_T = 1$ bps/Hz, $\Gamma_1 = \Gamma_2 = \cdots = \Gamma_N = \Gamma$ (dB))

equalizers considered, the MMSE-DFE performs better.

Chapter 4

CONCLUSIONS AND FUTURE RESEARCH

In this chapter first we present the conclusions and then we discuss the future scope for research in areas related to multi-hop amplify-and-forward full-duplex relaying system and we briefly discuss the scenarios where MGF approach simplifies the procedure in finding the input-output relationship of such a system.

4.1 Conclusions

In Chapter 2 of this thesis, we proposed a signal flow graph approach to find the z-transform domain input-output relationship of a multi-hop full-duplex amplify-and-forward network by using MGF. This approach provides an easy method to find the input-output relationship compared to the conventional recursive substitution method which is tedious and complex especially when the end-to-end system has many relays with inter-relay interference. Using this transform domain input-output relationship we derived a generalized end-to-end effective channel equations with the information signal and the noise inputs.

In Chapter 3 of this thesis, using the transform domain input-output relationship, we derived the output SNR of different types of equalizers and matched filter at the destination. Using the output SNR we performed the outage probability analysis of a multi-hop full-duplex amplify-and-forward system with tow-hops and three-hops. For the case of a three-hop system, we showed that the full-duplex amplify-and-forward network performs better than the half-duplex amplify-and-forward network for high target rates. Also, by considering different types of equalizers at the destination to deal with the frequency-selective channel introduced by full-duplex relaying and

matched filtering, we showed in simulations that, as the strength of RSI signal increases, the outage probability of the end-to-end system also increases. Finally, for the case of a three-hop network, by assuming perfect self-interference cancellation in one the relay at a time, we simulated the lower bounds on the outage probability of the end-to-end system and saw that they are tight for the three-hop example.

4.2 Future Works

Further works are discussed in the following subsections:

4.2.1 Continuous-time System Model

Instead of the discrete-time system model, one can consider a continuous-time system model and still use the signal flow graph approach to find the effective channels for information signal and noise at the destination of a multi-hop full-duplex amplify-and-forward relaying system. One can consider processing delay e^{-sT}, where T is the processing time at the relays and propagation delay $e^{-s\tau_i}, i = 1, ..., N-1$, between i^{th} and $(i+1)^{th}$ relays. $e^{-s\tau_0}$ is the propagation delays between the source and R_1 and $e^{-s\tau_N}$ is the propagation delays between R_N and the destination. The corresponding signal flow graph is shown in figure 4.1.

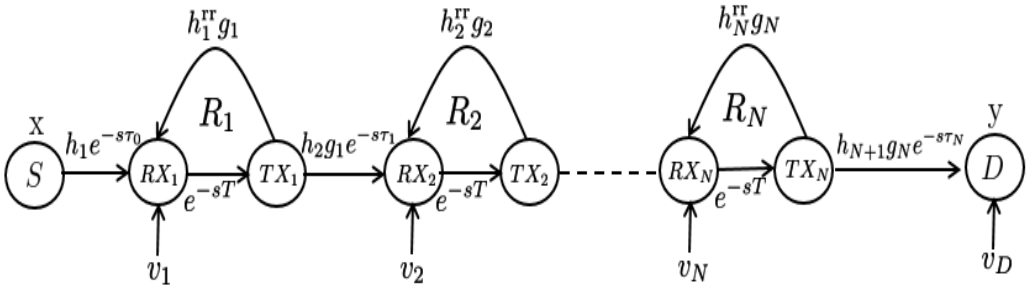

Figure 4.1: Signal-flow Graph of Continuous-time System Model

The transfer function of the system from S to D corresponding to the input signal can be obtained from the signal flow graph given in Fig. 4.1, using Mason's gain

formula as,

$$H(s) = \frac{h_1 e^{-NsT} \prod_{k=1}^{N} h_{k+1} g_k e^{-s\left(\sum_{m=0}^{N} \tau_k\right)}}{1 + \sum_{k=1}^{N} e^{-ksT} (-1)^k \sum_{A \in \mathbb{S}_k} \prod_{j \in A} h_j^{rr} g_j}. \tag{4.1}$$

Here $\mathbb{S}_k$ represents set of all the non-empty subsets of $\{1, 2, ..., N\}$ with k elements. Following a similar procedure as in the previous case, the transfer function of the system describing the input-output relationship corresponding to i^{th} noise input v_i at the relay R_i can be formulated as,

$$H_{\mathrm{n}i}(s) = \frac{h_1 e^{-sT(N-i-1)} \prod_{k=i}^{N} h_{k+1} g_k e^{-s\left(\sum_{m=i}^{N} \tau_k\right)}}{1 + \sum_{k=1}^{N} e^{-ksT} (-1)^k \sum_{A \in \mathbb{S}_k} \prod_{j \in A} h_j^{rr} g_j}. \tag{4.2}$$

Here $\mathbb{S}_{k,i}$ represents set of all the non-empty subsets of $\{i, ..., N\}$ with k elements.

Spectral densities of input signal and noise can we obtained from (4.1) and (4.2) respectively and the outage probability analysis can be performed similarly to the analysis we performed in Chapter. 3.

4.2.2 Outage Probability Analysis of MIMO Systems

Our signal flow graph approach to finding the input-output relationship of a multi-hop full-duplex amplify-and-forward relaying system can be extended to find the input-output relationship of multiple-input and multiple-output (MIMO) systems.

Consider a MIMO system as shown in Fig. 4.2. The relay has RSI term h_{ij}^{rr}, $i = 1, \cdots, t$ represents a transmitting antenna, $j = 1, \cdots, r$ represents a receiving antenna, h_{ij} represents an inter-relay channel from the source to the relay, h_{ij}^{R} represents an inter-relay channel from the relay to the destination and g represents the

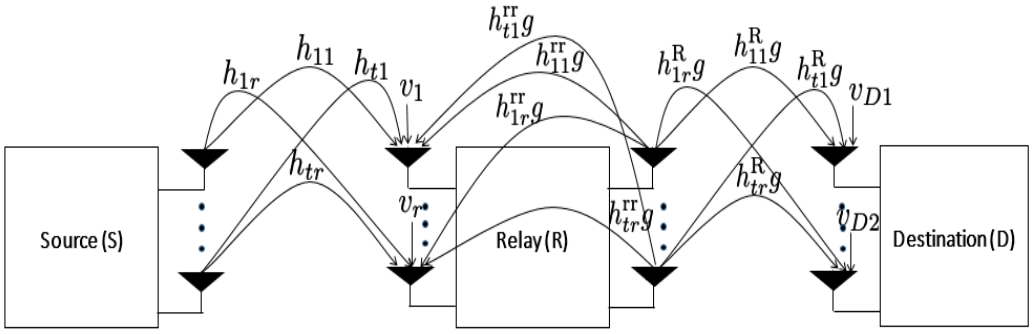

Figure 4.2: MIMO System Model

amplification factor at the relay. By writing the corresponding signal-flow graph of the MIMO system model, one can use the Mason's gain formula to perform the outage probability analysis.

MIMO relays usually incorporate a precoding stage in order to improve reception quality. Normally, these precoders are designed assuming that there is no self-interference, resulting in a serious performance loss if interference is not sufficiently mitigated. Authors in [40] proposed a spatio-temporal approach to the problem of self-interference mitigation at full-duplex amplify-and-forward MIMO relays. Their approach can deal with frequency-selective channels by exploiting the knowledge of the auto-correlation of the useful transmitted signal from the main transmitter, thus providing the relay protocol with an interference-free signal.

4.2.3 Ergodic Capacity of Multi-hop Amplify-and-forward Full-duplex Relaying Systems

Using the output SNR expression assuming a matched filter or an equalizer at the destination, one can calculate the ergodic capacity, $E(C)$, of the multi-hop full-duplex amplify-and-forward relaying system by using the relationship: $E(C) = E\left[\log_2\left(1 + \gamma_{\text{output}}\right)\right]$, where, γ_{output} represents the end-to-end output SNR expression. Also, one can use Jensen's inequality to derive the bounds on the ergodic capacity.

4.2.4 Diversity Analysis in Amplify-and-forward Full-duplex Systems with Frequency-selective Fading Channels

Mathematical proofs of MMSE equalizer and MMSE-DFE taking advantage of diversity in frequency-selective fading channels can be derived for a multi-hop full-duplex amplify-and-forward relaying system.

4.2.5 Outage Probability Analysis Assuming Different Fading Models

Outage probability analysis can be performed by assuming Rician or Nakagami-m fading models. In our thesis we have assumed that the line of sight component of self-interference is mitigated by passive isolation techniques, therefore, the RSI fading channel is Rayleigh distributed. But, the experiments in [38] have shown that the most realistic model for RSI channel is the Rician fading model with low K-factor (about -10dB to 10dB).

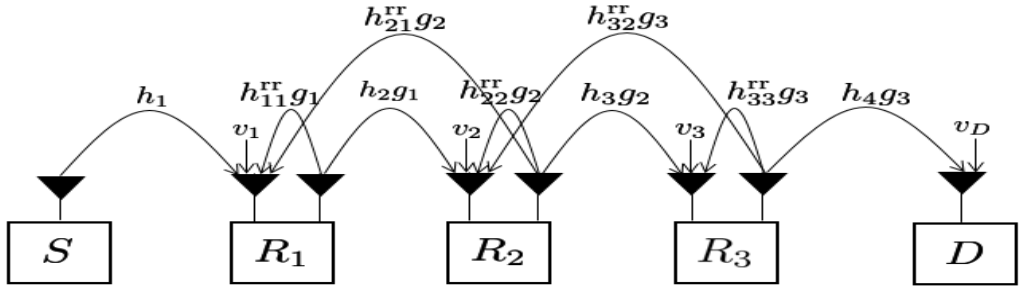

Figure 4.3: Three Relay System with Inter-relay Interference

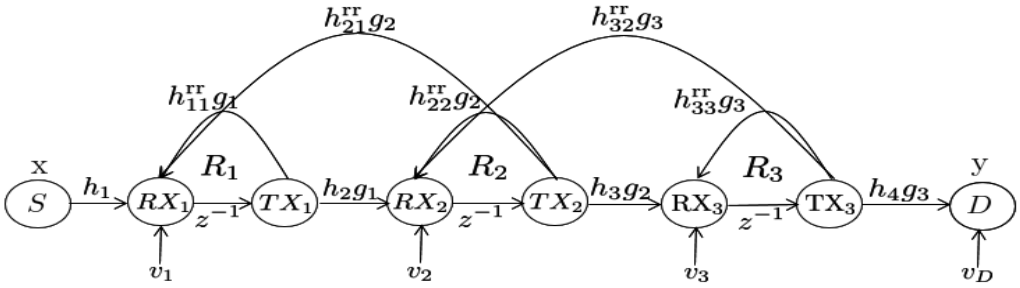

Figure 4.4: Signal-flow Graph of Three Relay System with Inter-relay Interference

4.2.6 Input-output Relationship of Multi-hop Relaying System with Inter-relay Interference

One can consider the interference from the neighboring relays (inter-relay interference) in the system model and outage probability analysis of such a system can be performed using the signal flow graph approach . As an example of such a system model, a three relay system with inter-relay interference is shown in Fig. 4.3 and the corresponding signal flow graph is as shown in Fig 4.4.

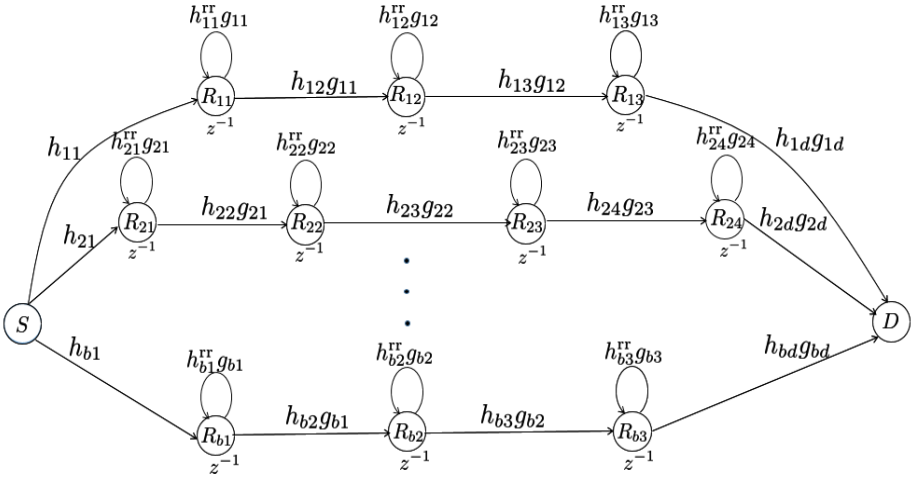

Figure 4.5: Signal-flow Graph of a System with Multi-hop Relays in Parallel

4.2.7 Input-output Relationship of a System with Multi-hops in Parallel

Consider a system with multi-hop relays in parallel as shown in Fig. 4.5, where, R_{ij} represents a relay with RSI term h_{ij}^{rr}, h_{ij} represents a inter-relay channel and g_{ij} represents the amplification factor at the R_{ij}^{th} relay, each j corresponds to a relay in i^{th} parallel branch. There can be inter-relay interference from the relays in the same parallel branch or from different branch which are not shown in Fig. 4.5. One can use the Mason's gain formula to find the transfer function of the end-to-end system, using which outage performance of the system can be studied.

REFERENCES

[1] A. Goldsmith, *Wireless communications*. Cambridge university press, 2005.

[2] M. Nakagami, "The m-distribution-A general formula of intensity distribution of rapid fading," *Statistical Method of Radio Propagation*, 1960.

[3] M. K. Simon and M.-S. Alouini, *Digital communication over fading channels*. John Wiley & Sons, 2005, vol. 95.

[4] P. Gupta and P. Kumar, "Towards an information theory of large networks: An achievable rate region," *IEEE Transactions on Information Theory*, vol. 49, no. 8, pp. 1877–1894, 2003.

[5] L.-L. Xie and P. R. Kumar, "An achievable rate for the multiple level relay channel," in *Information Theory, 2004. ISIT 2004. Proceedings. International Symposium on*. IEEE, 2004, p. 3.

[6] G. Kramer, M. Gastpar, and P. Gupta, "Cooperative strategies and capacity theorems for relay networks," *IEEE Transactions on Information Theory*, vol. 51, no. 9, pp. 3037–3063, 2005.

[7] H. Bolcskei, R. U. Nabar, O. Oyman, and A. J. Paulraj, "Capacity scaling laws MIMO relay networks," *IEEE Transactions on Wireless Communications*, vol. 5, no. 6, pp. 1433–1444, 2006.

[8] P. Gupta and P. R. Kumar, "The capacity of wireless networks," *IEEE Transactions on information theory*, vol. 46, no. 2, pp. 388–404, 2000.

[9] M. Gastpar and M. Vetterli, "On the capacity of wireless networks: The relay case," in *INFOCOM 2002. Twenty-First Annual Joint Conference of the IEEE Computer and Communications Societies. Proceedings. IEEE*, vol. 3. IEEE, 2002, pp. 1577–1586.

[10] A. Host-Madsen and J. Zhang, "Capacity bounds and power allocation for wireless relay channels," *IEEE transactions on Information Theory*, vol. 51, no. 6, pp. 2020–2040, 2005.

[11] R. Pabst, B. H. Walke, D. C. Schultz, P. Herhold, H. Yanikomeroglu, S. Mukherjee, H. Viswanathan, M. Lott, W. Zirwas, M. Dohler *et al.*, "Relay-based deployment concepts for wireless and mobile broadband radio," *IEEE Communications Magazine*, vol. 42, no. 9, pp. 80–89, 2004.

[12] J. Laneman, D. Tse, and G. W. Wornell, "Cooperative diversity in wireless networks: Efficient protocols and outage behavior," *IEEE Transactions on Information Theory*, vol. 50, no. 12, pp. 3062–3080, Dec 2004.

[13] M. O. Hasna and M. S. Alouini, "End-to-end performance of transmission systems with relays over Rayleigh-fading channels," *IEEE Transactions on Wireless Communications*, vol. 2, no. 6, pp. 1126–1131, Nov 2003.

[14] C. Jeong, B. Seo, S. R. Lee, H. M. Kim, and I. M. Kim, "Relay precoding for non-regenerative MIMO relay systems with partial CSI feedback," *IEEE Transactions on Wireless Communications*, vol. 11, no. 5, pp. 1698–1711, May 2012.

[15] R. Pabst, B. H. Walke, D. C. Schultz, P. Herhold, H. Yanikomeroglu, S. Mukherjee, H. Viswanathan, M. Lott, W. Zirwas, M. Dohler, H. Aghvami, D. D. Falconer, and G. P. Fettweis, "Relay-based deployment concepts for wireless and mobile broadband radio," *IEEE Communications Magazine*, vol. 42, no. 9, pp. 80–89, Sept 2004.

[16] R. U. Nabar, H. Bolcskei, and F. W. Kneubuhler, "Fading relay channels: Performance limits and space-time signal design," *IEEE Journal on Selected Areas in Communications*, vol. 22, no. 6, pp. 1099–1109, Aug 2004.

[17] X. J. Zhang and Y. Gong, "Adaptive power allocation for regenerative relaying with multiple antennas at the destination," *IEEE Transactions on Wireless Communications*, vol. 8, no. 6, pp. 2789–2794, June 2009.

[18] J. Kaleva, A. Tlli, and M. Juntti, "User admission for multi-user regenerative relay MIMO systems," in *2013 IEEE International Conference on Communications (ICC)*, June 2013, pp. 5850–5854.

[19] A. Otyakmaz, R. Schoenen, S. Dreier, and B. H. Walke, "Parallel operation of half- and full-duplex FDD in future multi-hop mobile radio networks," in *Wireless Conference, 2008. EW 2008. 14th European*, June 2008, pp. 1–7.

[20] T. Riihonen, S. Werner, and R. Wichman, "Comparison of full-duplex and half-duplex modes with a fixed amplify-and-forward relay," in *Wireless Communications and Networking Conference, 2009. WCNC 2009. IEEE*, April 2009, pp. 1–5.

[21] D. Soldani and S. Dixit, "Wireless relays for broadband access [radio communications series]," *IEEE Communications Magazine*, vol. 46, no. 3, pp. 58–66, March 2008.

[22] A. Sabharwal, P. Schniter, D. Guo, D. Bliss, S. Rangarajan, and R. Wichman, "In-band full-duplex wireless: Challenges and opportunities," *IEEE Journal on Selected Areas in Communications*, vol. 32, no. 9, pp. 1637–1652, Sept 2014.

[23] D. Kim, H. Lee, and D. Hong, "A survey of in-band full-duplex transmission: From the perspective of PHY and MAC layers," *IEEE Communications Surveys Tutorials*, vol. PP, no. 99, pp. 1–1, 2015.

[24] S. Hong, J. Brand, J. Choi, M. Jain, J. Mehlman, S. Katti, and P. Levis, "Applications of self-interference cancellation in 5G and beyond," *IEEE Communications Magazine*, vol. 52, no. 2, pp. 114–121, February 2014.

[25] C. Li, X. Wang, L. Yang, and W.-P. Zhu, "A joint source and relay power allocation scheme for a class of MIMO relay systems," *IEEE Transactions on Signal Processing*, vol. 57, no. 12, pp. 4852–4860, 2009.

[26] H. Ju, E. Oh, and D. Hong, "Improving efficiency of resource usage in two-hop full duplex relay systems based on resource sharing and interference cancellation," *IEEE Transactions on Wireless Communications*, vol. 8, no. 8, pp. 3933–3938, 2009.

[27] M. A. Khojastepour, K. Sundaresan, S. Rangarajan, X. Zhang, and S. Barghi, "The case for antenna cancellation for scalable full-duplex wireless communications," in *Proceedings of the 10th ACM Workshop on Hot Topics in Networks*. ACM, 2011, p. 17.

[28] T. Riihonen, S. Werner, and R. Wichman, "Spatial loop interference suppression in full-duplex MIMO relays," in *Signals, Systems and Computers, 2009 Conference Record of the Forty-Third Asilomar Conference on*. IEEE, 2009, pp. 1508–1512.

[29] T. Riihonen, S. Werner, R. Wichman, and Z. Eduardo, "On the feasibility of full-duplex relaying in the presence of loop interference," in *Signal Processing Advances in Wireless Communications, 2009. SPAWC '09. IEEE 10th Workshop on*, June 2009, pp. 275–279.

[30] V. R. Cadambe and S. A. Jafar, "Degrees of freedom of wireless networks with relays, feedback, cooperation, and full duplex operation," *IEEE Transactions on Information Theory*, vol. 55, no. 5, pp. 2334–2344, 2009.

[31] M. Jain, J. I. Choi, T. Kim, D. Bharadia, S. Seth, K. Srinivasan, P. Levis, S. Katti, and P. Sinha, "Practical, real-time, full duplex wireless," in *Proceedings of the 17th annual international conference on Mobile computing and networking*. ACM, 2011, pp. 301–312.

[32] J. I. Choi, M. Jain, K. Srinivasan, P. Levis, and S. Katti, "Achieving single channel, full duplex wireless communication," in *Proceedings of the sixteenth annual international conference on Mobile computing and networking*. ACM, 2010, pp. 1–12.

[33] M. Duarte and A. Sabharwal, "Full-duplex wireless communications using off-the-shelf radios: Feasibility and first results," in *Signals, Systems and Computers (ASILOMAR), 2010 Conference Record of the Forty Fourth Asilomar Conference on*, Nov 2010, pp. 1558–1562.

[34] D. Bharadia, E. McMilin, and S. Katti, "Full duplex radios," in *ACM SIGCOMM Computer Communication Review*, vol. 43, no. 4. ACM, 2013, pp. 375–386.

[35] D. Bharadia and S. Katti, "Full duplex MIMO radios," in *11th USENIX Symposium on Networked Systems Design and Implementation (NSDI 14)*, 2014, pp. 359–372.

[36] D. Bharadia and S. Katti, "Fastforward: Fast and constructive full duplex relays," vol. 44, no. 4, pp. 199–210, 2014.

[37] B. Day, A. Margetts, D. Bliss, and P. Schniter, "Full-duplex bidirectional MIMO: Achievable rates under limited dynamic range," *IEEE Transactions on Signal Processing*, vol. 60, no. 7, pp. 3702–3713, July 2012.

[38] M. Duarte, C. Dick, and A. Sabharwal, "Experiment-driven characterization of full-duplex wireless systems," *IEEE Transactions on Wireless Communications*, vol. 11, no. 12, pp. 4296–4307, 2012.

[39] T. M. Kim and A. Paulraj, "Outage probability of amplify-and-forward cooperation with full duplex relay," in *2012 IEEE Wireless Communications and Networking Conference (WCNC)*, April 2012, pp. 75–79.

[40] E. Antonio-Rodriguez, R. Lopez-Valcarce, T. Riihonen, S. Werner, and R. Wichman, "Autocorrelation-based adaptation rule for feedback equalization in wideband full-duplex amplify-and-forward MIMO relays," in *Acoustics, Speech and Signal Processing (ICASSP), 2013 IEEE International Conference on*, May 2013, pp. 4968–4972.

[41] J. Ma, G. Y. Li, J. Zhang, T. Kuze, and H. Iura, "A new coupling channel estimator for cross-talk cancellation at wireless relay stations," in *Global Telecommunications Conference, 2009. GLOBECOM 2009. IEEE.* IEEE, 2009, pp. 1–6.

[42] A. Masmoudi and T. Le-Ngoc, "A maximum-likelihood channel estimator for self-interference cancellation in full-duplex systems," 2015.

[43] T. Riihonen, S. Werner, and R. Wichman, "Mitigation of loopback self-interference in full-duplex MIMO relays," *IEEE Transactions on Signal Processing*, vol. 59, no. 12, pp. 5983–5993, 2011.

[44] L. Jimenez Rodriguez, N. Tran, and T. Le-Ngoc, "Performance of full-duplex AF relaying in the presence of residual self-interference," *IEEE Journal on Selected Areas in Communications*, vol. 32, no. 9, pp. 1752–1764, Sept 2014.

[45] T. Riihonen, S. Werner, and R. Wichman, "Residual self-interference in full-duplex MIMO relays after null-space projection and cancellation," in *2010 Conference Record of the Forty Fourth Asilomar Conference on Signals, Systems and Computers.* IEEE, 2010, pp. 653–657.

[46] R. Hu, M. Peng, Z. Zhao, and X. Xie, "Investigation of full-duplex relay networks with imperfect channel estimation," in *2014 IEEE/CIC International Conference on Communications in China (ICCC).* IEEE, 2014, pp. 576–580.

[47] B. Chun and Y. H. Lee, "A spatial self-interference nullification method for full duplex amplify-and-forward MIMO relays," in *2010 IEEE Wireless Communication and Networking Conference.* IEEE, 2010, pp. 1–6.

[48] E. Everett, A. Sahai, and A. Sabharwal, "Passive self-interference suppression for full-duplex infrastructure nodes," *IEEE Transactions on Wireless Communications*, vol. 13, no. 2, pp. 680–694, February 2014.

[49] E. Aryafar, M. A. Khojastepour, K. Sundaresan, S. Rangarajan, and M. Chiang, "Midu: Enabling MIMO full duplex," in *Proceedings of the 18th annual international conference on Mobile computing and networking*. ACM, 2012, pp. 257–268.

[50] A. K. Khandani, "Methods for spatial multiplexing of wireless two-way channels," Oct. 19 2010, uS Patent 7,817,641.

[51] E. Everett, "Full-duplex infrastructure nodes: Achieving long range with half-duplex mobiles," Ph.D. dissertation, Rice University, 2012.

[52] E. Everett, M. Duarte, C. Dick, and A. Sabharwal, "Empowering full-duplex wireless communication by exploiting directional diversity," in *2011 Conference Record of the Forty Fifth Asilomar Conference on Signals, Systems and Computers (ASILOMAR)*, Nov 2011, pp. 2002–2006.

[53] M. Duarte, C. Dick, and A. Sabharwal, "Experiment-driven characterization of full-duplex wireless systems," *IEEE Transactions on Wireless Communications*, vol. 11, no. 12, pp. 4296–4307, 2012.

[54] M. Duarte, A. Sabharwal, V. Aggarwal, R. Jana, K. K. Ramakrishnan, C. W. Rice, and N. K. Shankaranarayanan, "Design and characterization of a full-duplex multiantenna system for wifi networks," *IEEE Transactions on Vehicular Technology*, vol. 63, no. 3, pp. 1160–1177, March 2014.

[55] S.-N. Hong, I. Maric, D. Hui, and G. Caire, "Multihop virtual full-duplex relay channels," in *Information Theory Workshop (ITW), 2015 IEEE*. IEEE, 2015, pp. 1–5.

[56] S.-N. Hong and G. Caire, "Virtual full-duplex relaying with half-duplex relays," *IEEE Transactions on Information Theory*, vol. 61, no. 9, pp. 4700–4720, Sept 2015.

[57] X. Li, "Optimal relay selection for transmission rate maximisation in multi-hop wireless networks," *Electronics Letters*, vol. 51, no. 12, pp. 949–950, 2015.

[58] J.-H. Lee, "Full-duplex relay for enhancing physical layer security in multi-hop relaying systems," *IEEE Communications Letters*, vol. 19, no. 4, pp. 525–528, April 2015.

[59] E. Everett, D. Dash, C. Dick, and A. Sabharwal, "Self-interference cancellation in multi-hop full-duplex networks via structured signaling," in *Communication, Control, and Computing (Allerton), 2011 49th Annual Allerton Conference on*. IEEE, 2011, pp. 1619–1626.

[60] A. Sadeghi, S. Mosavat-Jahromi, F. Lahouti, and M. Zorzi, "Multi-hop wireless transmission with half duplex and imperfect full duplex relays," in *Telecommunications (IST), 2014 7th International Symposium on*, Sept 2014, pp. 1026–1029.

[61] Q. Li, K. Li, and K. Teh, "Achieving optimal diversity-multiplexing tradeoff for full-duplex MIMO multihop relay networks," *IEEE Transactions on Information Theory*, vol. 57, no. 1, pp. 303–316, Jan 2011.

[62] Y. Sugiyama, K. Tamaki, S. Saruwatari, and T. Watanabe, "A wireless full-duplex and multi-hop network with collision avoidance using directional antennas," in *Mobile Computing and Ubiquitous Networking (ICMU), 2014 Seventh International Conference on*, Jan 2014, pp. 38–43.

[63] Y. Yang and N. B. Shroff, "Scheduling in wireless networks with full-duplex cut-through transmission."

[64] K. Tamaki, H. Ari Raptino, Y. Sugiyama, M. Bandai, S. Saruwatari, and T. Watanabe, "Full duplex media access control for wireless multi-hop networks," in *Vehicular Technology Conference (VTC Spring), 2013 IEEE 77th*, June 2013, pp. 1–5.

[65] T. Baranwal, D. Michalopoulos, and R. Schober, "Outage analysis of multihop full duplex relaying," *IEEE Communications Letters*, vol. 17, no. 1, pp. 63–66, January 2013.

[66] S. Han, C.-L. I, Z. Xu, C. Pan, and Z. Pan, "Full duplex: Coming into reality in 2020?" in *Global Communications Conference (GLOBECOM), 2014 IEEE*, Dec 2014, pp. 4776–4781.

[67] N. Mahmood, G. Berardinelli, F. Tavares, and P. Mogensen, "On the potential of full duplex communication in 5G small cell networks," in *Vehicular Technology Conference (VTC Spring), 2015 IEEE 81st*, May 2015, pp. 1–5.

[68] Z. Zhang, X. Chai, K. Long, A. Vasilakos, and L. Hanzo, "Full duplex techniques for 5G networks: self-interference cancellation, protocol design, and relay selection," *IEEE Communications Magazine*, vol. 53, no. 5, pp. 128–137, May 2015.

[69] X. Zhang, W. Cheng, and H. Zhang, "Heterogeneous statistical qos provisioning over 5G mobile wireless networks," *IEEE Network*, vol. 28, no. 6, pp. 46–53, Nov 2014.

[70] I. Krikidis, H. Suraweera, S. Yang, and K. Berberidis, "Full-duplex relaying over block fading channel: A diversity perspective," *IEEE Transactions on Wireless Communications*, vol. 11, no. 12, pp. 4524–4535, December 2012.

[71] C. Coates, "Flow-graph solutions of linear algebraic equations," *IRE Transactions on Circuit Theory*, vol. 6, no. 2, pp. 170–187, Jun 1959.

[72] S. Mason, "Feedback theory-further properties of signal flow graphs," *Proceedings of the IRE*, vol. 44, no. 7, pp. 920–926, July 1956.

[73] R. C. Dorf and R. H. Bishop, *Modern Control Systems*, 12th ed. NJ: Prentice Hall, 2011.

[74] K. C. Dheeraj, A. Thangaraj, and R. Ganti, "Equalization in amplify-forward full-duplex relay with direct link," in *Communications (NCC), 2015 Twenty First National Conference on*, Feb 2015, pp. 1–6.

[75] J. G. Proakis and M. Salehi, *Digital Communications*, 5th ed. NY: McGraw-Hill, 2008.

[76] I. S. Gradshteyn and I. M. Ryzhik, *Table of integrals, series, and products*. Academic press, 2014.

[77] J. M. Cioffi, G. P. Dudevoir, M. V. Eyuboglu, and G. D. Forney, "MMSE decision-feedback equalizers and coding. i. equalization results," *IEEE Transactions on Communications*, vol. 43, no. 10, pp. 2582–2594, Oct 1995.

[78] M. Hasna and M.-S. Alouini, "Outage probability of multihop transmission over Nakagami fading channels," *IEEE Communications Letters*, vol. 7, no. 5, pp. 216–218, May 2003.